Helsinki University of Technology
Inorganic Chemistry Publication Series
Espoo 2004 No. 7

ATOMIC LAYER DEPOSITION OF BINARY AND TERNARY LEAD AND BISMUTH OXIDE THIN FILMS

Jenni Harjuoja

Dissertation for the degree of Doctor of Science in Technology to be presented with due permission of the Department of Chemical Technology for public examination and debate in Auditorium KE 2 at Helsinki University of Technology (Espoo, Finland) on the 27th of April, 2007, at 12 noon.

Helsinki University of Technology
Department of Chemical Technology
Laboratory of Inorganic and Analytical Chemistry

Teknillinen korkeakoulu
Kemian tekniikan osasto
Epäorgaanisen ja analyyttisen kemian laboratorio

Supervisor:

Prof. Lauri Niinistö
Laboratory of Inorganic and Analytical Chemistry
Helsinki University of Helsinki

Pre-Examiners:

Prof. Cheol-Seong Hwang
School of Material Science and Engineering
Seoul National University, Korea

Dr. Mikael Schuisky
Sandvik AB
Sandviken, Sweden

Opponent:

Dr. Ola Nilsen
Department of Chemistry
University of Oslo, Norway

Distribution:
Helsinki University of Technology
Laboratory of Inorganic and Analytical Chemistry
P.O. Box 6100
FIN-02150 TKK, FINLAND

ISBN 978-951-22-8702-4 (Printed)
ISBN 978-951-22-8703-1 (Electronic)
http://lib.tkk.fi/Diss/index.htm
ISSN 1458-5154

Otamedia Oy
Espoo 2007

ABSTRACT

This thesis describes the deposition of binary lead oxide and ternary lead titanate, lead zirconate, bismuth silicate, and bismuth titanate films by atomic layer deposition (ALD) and characterization of structural, compositional and surface properties of the films. The first part of the thesis reviews the principles of the ALD technique and the relevant literature on perovskite oxides and films and the deposition of lead and bismuth films by ALD, and the second part summarizes the experimental work reported in the five appended publications.

On the basis of the binary lead oxide depositions, the Ph_4Pb/O_3 process was chosen for the ternary oxide studies. Careful optimization of the pulsing ratio of the binary oxides allowed processing of stoichiometric perovskite $PbTiO_3$ and $PbZrO_3$ thin films. Crystalline $PbTiO_3$ on Si(100) was detected after annealing at 600 °C. In the case of lead zirconate, the perovskite phase ($PbZrO_3$) was obtained on $SrTiO_3$(100) after annealing at 600 °C. In both cases, a slight excess of lead enhanced the crystallinity. Roughness values were nevertheless higher than values obtained in binary processes.

A new bimetallic precursor $Bi(CH_2SiMe_3)_3$ was introduced for the deposition of bismuth silicate. With ozone as oxidizing agent, ALD-window for Bi-Si-O thin film growth was found at 250-350 °C. The Si to Bi atomic ratio in this region was about 2. Addition of a second bismuth precursor, $BiPh_3$, increased the bismuth content. Combination of the $BiPh_3/O_3$ process and the $Ti(O\text{-}i\text{-}Pr)_4/H_2O$ process allowed successful deposition of bismuth titanate. Good control of the film stoichiometry was achieved at the deposition temperature of 250 °C.

Both as-deposited ternary bismuth oxides were amorphous. After annealing at 600 °C, the a-axis-oriented Bi_2SiO_5 phase was detected. Higher annealing temperatures were necessary for bismuth titanate. The most textured film of $Bi_4Ti_3O_{12}$ was obtained in N_2 atmosphere at annealing temperature of 1000 °C. Roughness values of the thin films were reasonable, being in the range of 0.3-1.3 nm.

PREFACE

This work was carried out between 2002 and 2006 in the Laboratory of Inorganic and Analytical Chemistry, Helsinki University of Technology. During these years I had the opportunity to work with many wonderful people to whom I would like to express my deepest gratitude.

Especially I want to express my sincere gratitude to Dr. Matti Putkonen for his invaluable guidance, help, and expert advice. Equally I am grateful to my supervisor, Professor Lauri Niinistö, for giving the opportunity to join the ALD group, and for his endless support and advice.

Warm thanks are extended to my co-others, and especially to Lic.Sci. (Tech.) Anne Kosola for her professional input to my thesis and for great company as an office mate; to Mr. Samuli Väyrynen and Dr. Eero Rauhala for the RBS measurements and help with the interpretation of the results; to Dr. Timo Sajavaara for performing the TOF-ERD analyses; to Dr. Jaakko Niinistö for guidance with AFM; to Professor Pekka Hautojärvi for providing the facilities for the AFM measurements, and to Mr. Marko Vehkamäki for performing the electrical measurements and fruitful discussion in our area of common interest. Mrs. Anita Pirhonen and Mr. Pekka Hassinen are thanked for their technical assistance.

Most importantly, I wish to thank my family, and particularly my husband Matti for his patience and constant support. Our little daughter Milla played a special role in reminding me of the true priorities of life.

Financial support from the Graduate School of Inorganic Materials Chemistry, the Jenny and Antti Wihuri Foundation, the Heikki and Hilma Honkanen Foundation, the Finnish Foundation for Economic and Technology Sciences (KAUTE) and the Foundation of Technology (TES) is gratefully acknowledged.

Espoo, February 2007

Jenni Harjuoja

LIST OF PUBLICATIONS

This thesis is based on the following original publications, which are referred to in the text by their Roman numerals I-V.

I Harjuoja, J., Putkonen, M., and Niinistö, L., Exploiting volatile lead compounds as precursors for the atomic layer deposition growth of lead dioxide thin films,
Thin Solid Films **497** (2006) 77-82.

II Harjuoja, J., Kosola, A., Putkonen, M., and Niinistö L., Atomic layer deposition and post-deposition annealing of $PbTiO_3$ thin films,
Thin Solid Films **496** (2006) 346-352.

III Harjuoja, J., Väyrynen, S., Putkonen, M., Niinistö, L., and Rauhala E., Atomic layer deposition of $PbZrO_3$ thin films,
Appl. Surf. Sci. **253** (2007) 5228-5232.

IV Harjuoja, J., Hatanpää, T., Vehkamäki, M., Väyrynen, S., Putkonen, M., Niinistö, L., Ritala, M., Leskelä, M., and Rauhala E., New approach to the ALD of bismuth silicates; $Bi(CH_2SiMe_3)_3$ acting as a precursor for both bismuth and silicon,
Chem. Vap. Deposition **11** (2005) 362-367.

V Harjuoja, J., Väyrynen, S., Putkonen, M., Niinistö, L., and Rauhala E., Crystallization of bismuth titanate and bismuth silicate grown as thin film by atomic layer deposition,
J. Cryst. Growth **286** (2006) 376-383.

THE AUTHOR'S CONTRIBUTION

Publication I	The research plan for the experimental work was drawn up together with Dr. Matti Putkonen. The author did the experimental work except for the TOF-ERD and AFM analyses, interpreted the results, and wrote the article.
Publication II	The author planned the research, and performed the experimental work except for the TOF-ERD analyses, post-deposition annealing, and characterization of annealed Pb-Ti-O films. The results were interpreted together with Lic.Sc. (Tech.) Anne Kosola and Dr. Matti Putkonen. The author had a major role in writing the article.
Publication III	The author did the research plan and the experimental work and interpreted the results except for the RBS and rocking curve measurements. The author wrote the article.
Publication IV	The author drew up the research plan and did the experimental work except for the precursor synthesis, analysis of the precursor, and the TOF-ERDA and RBS measurements. The author had a major role in writing the article.
Publication V	The research plan for the experimental work was defined together with Dr. Matti Putkonen. The author was responsible for most of the film depositions and for the analysis of the films except for the RBS analyses. The author interpreted the results and wrote the article.

LIST OF ABBREVIATIONS AND ACRONYMS

AES	Auger electron spectroscopy
AFM	Atomic force microscope/microscopy
ALD	Atomic layer deposition
BFO	Bismuth ferrite, $BiFeO_3$
BLT	Bismuth lanthanum titanate, $Bi_{4-x}La_xTi_3O_{12}$
Cp	Cyclopentadienyl, C_5H_5
CVD	Chemical vapor deposition
dedtc	Diethyl dithiocarbamate, $-S_2CNEt_2$
dmae	Diethylaminoethoxide, $-OCH_2CH_2NMe_2$
EL	Electroluminescence
Et	Ethyl, $-CH_2CH_3$
FeRAM	Ferroelectric random access memory
IC	Integrated circuits
IR	Infrared
^{i}Pr	Isopropyl, $-CH(CH_3)_2$
ME	Methoxyethoxide, $-OCH_2CH_2OMe$
Me	Methyl, $-CH_3$
MEMS	Micro-electromechanical systems
mmp	1-Methoxy-2-methyl-2-propoxide, $-OC(CH_3)_2CH_2OCH_3$
MOCVD	Metalorganic chemical vapor deposition
^{n}Bu	n-Butyl, $-(CH_2)_3CH_3$
Ph	Phenyl, $-C_6H_5$
PLZT	Lead lanthanum zirconium titanate, $(Pb_yLa_{1-y})(Zr_xTi_{1-x})O_3$
PZT	Lead zirconium titanate, $Pb(Zr_xTi_{1-x})O_3$
RBS	Rutherford back-scattering spectrometry
rms	Root mean square
SEM	Scanning electron microscopy
SBT	Strontium bismuth tantalate, $SrBi_2Ta_2O_9$
TG	Thermogravimetry
^{t}Bu	Tert-butyl, $-C(CH_3)_3$
TEM	Transmission electron microscopy
thd	2,2,6,6-Tetramethyl-3,5-heptanedione, $C_{11}H_{20}O_2$
TMA	Trimethylaluminum, $Al(CH_3)_3$
tmod	2,2,6,6-Tetramethyl-3,5-octanedionato, $C_{12}H_{21}O_2$
TOF-ERDA	Time-of-flight elastic recoil detection analysis
XPS	X-ray photoelectron spectroscopy
XRD	X-ray diffraction
XRF	X-ray fluorescence
YSZ	Yttrium-stabilized zirconium oxide

CONTENTS

1 Introduction

Many ternary and more complex oxides of lead and bismuth (e.g. $PbTiO_3$, $Bi_4Ti_3O_{12}$) crystallize in the perovskite structure. Perovskite oxides are an intriguing and highly attractive class of materials with a large range of properties and applications.[1] Traditionally they have been studied in bulk form, but their increased use in microelectronics and integration to silicon-based circuits are now putting the focus on thin film studies. [2] Besides ferroelectricity, the perovskites of interest in this thesis have been studied for their piezoelectricity, pyroelectricity, and electro-optic activity.[3] Furthermore some antiferroelectric materials based on the perovskite structure have been studied for possible thin film applications.[4]

Atomic layer deposition (ALD) is a vapor phase thin film deposition method. It has aroused great interest in the microelectronics industry, since high quality and accurately controlled thin films can be produced even in three-dimensional structures.[5] While the deposition of binary oxides is straightforward, the deposition of ternary and more complex oxides is demanding. First of all, it is difficult to find suitable precursors for all the metals. Furthermore the cation stoichiometry of multication thin films has to be accurately controlled to produce the desired material. Atomic layer deposition of multication films has not, therefore, been extensively studied.

Deposition of binary and ternary oxides of lead and bismuth by ALD was the task set for this work. The general properties of perovskite oxides and thin films are discussed in the first part of the literature reviews. Multicomponent precursors suitable for ALD are discussed, and the ALD of lead and bismuth compounds. The experimental part summarizes studies on lead oxide[I], lead titanate[II], lead zirconate[III], bismuth silicate[IV,V] and bismuth titanate[V] films deposited by ALD.

The purpose of this work was to demonstrate the ALD of ternary oxides of both lead and bismuth and to characterize the deposited films. In the case of lead oxide, the binary oxide was produced with use of different precursors.[I] After that, ternary lead titanate and lead zirconate depositions were demonstrated using one selected precursor combination.[II-III] Finally, studies on ternary bismuth systems, viz. bismuth silicate and bismuth titanate were carried out.[IV,V] Also, new bimetallic precursor for the deposition of bismuth silicate was reported.[IV] Together with careful study of growth parameters,

attention was paid to the effect of annealing on crystallinity, surface morphology, and diffusion. Although the ternary materials have potential uses in microelectronics because of their ferroelectric and other electric properties, the main goal of the work was to study new ternary processes for lead and bismuth. Electrical properties of the films were not studied, therefore.

2 Properties of perovskite oxides and perovskite thin films

The diverse chemical compositions and properties of the perovskite oxides provide a basic for wide-ranging research and applications. The electrical conductivity of perovskite oxides varies from insulating to semiconductive, metallic and even superconductive.[1] Besides interesting optical properties, they exhibit magnetism and catalytic activity.[2,6]

Probably the most important properties of perovskite thin films are their high dielectric constants and ferroelectric behavior, which are extensively exploited in microelectronics applications.[7,8] Capability for miniaturization and high performance together with special materials properties play a key role in these applications.

An introduction to perovskite chemistry and some special applications of thin film perovskite oxides are briefly presented below.

2.1 Structural chemistry of perovskite oxides

Properties of perovskite oxides are usually explained in terms of the perovskite structure ABO_3 (Figure 1a), where the A-cation is twelve- and the B-cation six-coordinated.[6] O is oxygen. The cubic perovskite structure consists of an A-cation, which sits in the center of the cube and is surrounded by corner-sharing BO_6 octahedra. Interesting properties arise when ternary perovskite-type oxide is more or less distorted from the ideal cubic structure.[1,6] Distortion of the perovskite structure can be described in terms of three different mechanisms: (i) cation displacements within the octahedra, (ii) distortions of the octahedral, and (iii) tilting of the octahedron.[9] An example of cation displacement is found in titanate-type ferroelectrics where the ferroelectricity originates from the two unequal $Ti\text{-}O^1$ and $Ti\text{-}O^2$ bond distances.[1] At a certain temperature, called the Curie temperature, this distortion transforms back to the cubic symmetry and ferroelectricity is lost. Both distortion and tilting of the octahedra have been observed in the $Bi_4Ti_3O_{12}$ structure where the mechanisms of ferroelectricity have been studied.[10] $Bi_4Ti_3O_{12}$ is one of the most interesting structures in the family of Aurivillius structures, where the Bi_2O_2 layers alternate with perovskite-like layers of $A_{n-1}B_nO_{3n+1}$ (Figure 1b).[11,12]

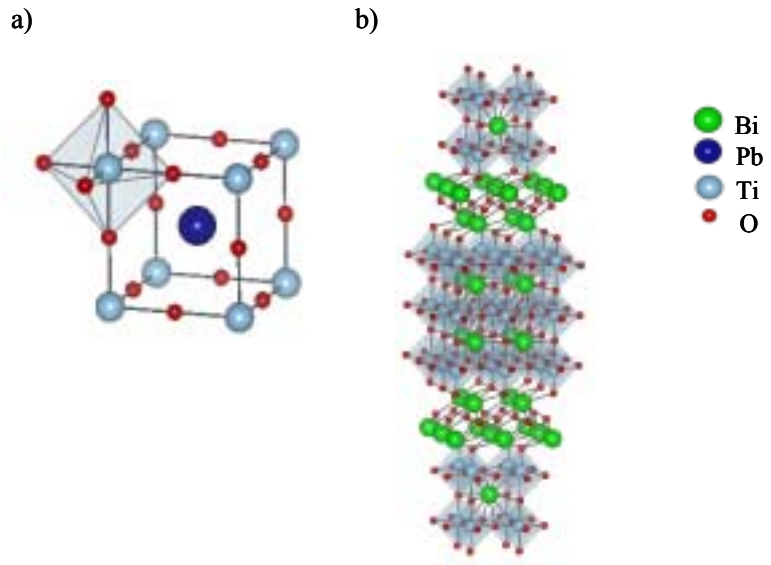

Figure 1. Simple perovskite structure for $PbTiO_3$ (a) and compared with an ideal Aurivillius structure for $Bi_4Ti_3O_{12}$ (b). Figures were drawn with VENUS.[13]

Variations of the ideal perovskite ABO_3 can be achieved by cation substitution. Changes in composition are usually accompanied by structural variations, and may improve the electrical and magnetic properties.[2] Most commonly this substitution is made at the cation site.

2.2 Perovskite materials as thin films

Most perovskite studies have dealt with bulk materials. However, perovskite films are of increasing interest because of their use in integrated circuits (IC).[2] Applications exploiting thin films offer a multitude of benefits, among them smaller size of the devices, better operating parameters and the facility for different shapes. Furthermore, materials that are difficult or even impossible to process in bulk form are in some cases easily processed in thin film form.[14] Thin film applications of perovskite materials represent a vast area, and only some of the more interesting applications can be summarized here. These applications relate to bismuth- and lead-based oxides, which are the focus of this thesis.

Ferroelectricity is one of the many interesting properties of perovskite oxides. The ferroelectric effect is an electrical phenomenon whereby some compounds exhibit a spontaneous polarization, which can be reversed by an electric field. When voltage is

applied to a perovskite crystal, for example to $PbTiO_3$, the relatively small titanium Ti^{4+} ion in the center of the cubic lattice is displaced relative to the oxygen octahedra.[2,3,15] This causes polarization of the crystal. Figure 2 illustrates the hysteresis behavior of polarization with electric field for a ferroelectric capacitor.

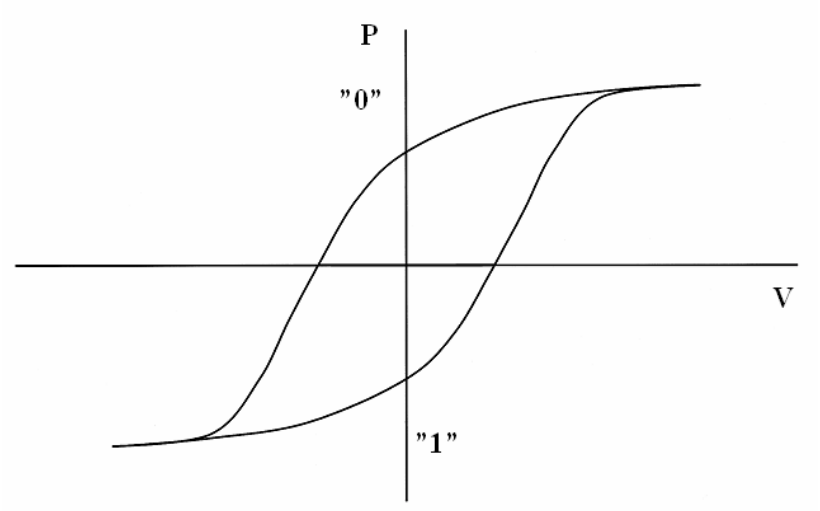

Figure 2. A typical ferroelectric hysteresis loop showing the two polarization states "0" and "1". P=polarization, V=voltage.

Depending on whether the voltage is positive or negative, the Ti^{4+} ion will move up or down, and thus it has two different polarization states (in Figure 2 illustrated as "0" and "1"). These two different polarization states enable the operation of non-volatile memories since when the voltage is switched off the polarization will remain. Non-volatile memory is one of the most intriguing features of ferroelectric materials. The most frequently studied materials for non-volatile memories are lead zirconium titanate ($Pb(Zr_xTi_{1-x})O_3$, PZT) and strontium bismuth tantalate ($SrBi_2Ta_2O_9$, SBT).[16,17] Related materials that have been studied for the same purpose are bismuth lanthanum titanate ($Bi_{4-x}La_xTi_3O_{12}$, BLT), and bismuth ferrite ($BiFeO_3$, BFO).[16]

Other studies are needed in parallel with the development of ferroelectric materials and new thin film deposition methods (i.e. ferroelectric material processing). In the case of PZT, it has been shown that ferroelectric degradation occurs when film thickness is decreased.[3] The recently developed novel electrode technology could prevent that.[18,19] In fact, ferroelectric memories with cell size of 0.27 μm^2 have already been demonstrated where the PZT thickness is as low as 70 nm.[18] Also, crystal orientation of

the ferroelectric needs to be controlled in order to provide homogeneous switching and increased polarization.[20] In the case of $Bi_4Ti_3O_{12}$, it has been shown that random orientation gives much better electrical properties than c-axis oriented film.[21]

Along with polarization, ferroelectric materials may show piezoelectricity, pyroelectricity, and electro-optic activity. As with polarization, structural changes are observed when voltage is applied across the ferroelectric layer. In the case of piezoelectricity, the thin film layer is compressed under the applied voltage, or electricity is generated in the thin film as a result of mechanical pressure.[2] When voltage is applied to a piezoelectric crystal, the crystal is distorted and the crystal axes become elongated. A polarized piezoelectric object is thus somewhat longer than it was before the voltage was applied. Many lead-based perovskites[22,23] and lanthanide-modified bismuth titanate[24-26] thin films have high piezoelectric coefficients and have been studied as micro-electromechanical systems (MEMS), suitable for use in actuators or pressure sensors, for example.[22-26]

As a result of change in the temperature, charges form on the surface of pyroelectric crystals. Thus, polarization of thin film structures changes with temperature, enabling the structures to be utilized as highly sensitive infrared detectors or as detector arrays in catalytic gas sensors. It should be noted that all pyroelectric materials are also piezoelectric, but not *vice versa*. While PZT[27-30] is the most widely studied perovskite material for pyroelectric applications, bismuth titanate[31] has aroused interest as well.

Electro-optical activity means that properties such as refractive indices or absorption properties change along with an applied voltage. Optical properties of bismuth- and lead-based ferroelectrics such as lanthanum-substituted bismuth titanate,[32] PZT,[33] and PLZT[34] have been extensively studied for exploitation in optical memories, optoelectronic devices, and waveguide applications.

The thicknesses of piezoelectric, pyroelectric, and electro-optic devices are usually in micrometer scale, but thicknesses below 1 μm have also been reported. Pyroelectric properties have been reported for 250 nm thin films, and electro-optical properties for even thinner films. Although in practise, it is not feasible to produce micrometer-scale

thin films by slow deposition methods like ALD, the method could perhaps find use in seed layer deposition.

3 ALD of Pb- and Bi-containing oxide thin films

Perovskite oxides are challenging materials for ALD. Depending on the material they consist of two or several cations, whose stoichiometry must be accurately controlled.[35] Finding compatible precursors so that requirements such as suitable deposition temperatures and growth rates are met is a demanding puzzle. These challenges are discussed in detail below. The basic principles of ALD are first reviewed (section 3.1). In the context of ALD and controlling the stoichiometry in complex oxide thin films, different alternatives for the precursor chemistry in the form of the bimetallic precursors are presented. Specifically, ALD processes based on lead and bismuth are discussed in section 3.3.

3.1 Principles of atomic layer deposition

Atomic layer deposition (ALD) is a sophisticated chemical vapor deposition (CVD) method for preparing thin films. ALD was developed in Finland[36] in the 1970s and has found wide acceptance and many applications.[5,37-41] Compared with conventional chemical vapor deposition methods, ALD is a low temperature method where thin films are deposited from the source vapors. Precursors are pulsed to the reaction chamber one at a time. In the case of binary oxides, growth typically proceeds in four steps. First the metal precursor is pulsed to the substrate surface, where it reacts with the surface groups, chemisorbing on the substrate. In the second step, non-reacted precursor species and gaseous reaction by-products are removed with an inert gas purge. An oxygen source is pulsed as second precursor in the third step to produce, by chemical reaction, the desired oxide material and at the same time releases remaining ligands from the metal precursor. The final step is the same as the second step. These four steps, forming one ALD growth cycle, are repeated as many times as necessary to obtain the desired film thickness. A schematic illustration of an ALD cycle is shown in Figure 3. Ideally during each metal precursor pulse, the substrate surface is covered with a full monolayer of the precursor, and surplus of the precursor is purged away in the following inert gas purge. Alternate pulsing of the precursors and saturative reactions enables a self-limiting growth. In practice, the limited number of reactive sites or bulky ligands of the metal precursor lead to less than monolayer growth. This can be

seen also in Figure 3, where for steric hindrances the large ML_3 molecules are unable to react with all –OH groups bound to the surface.

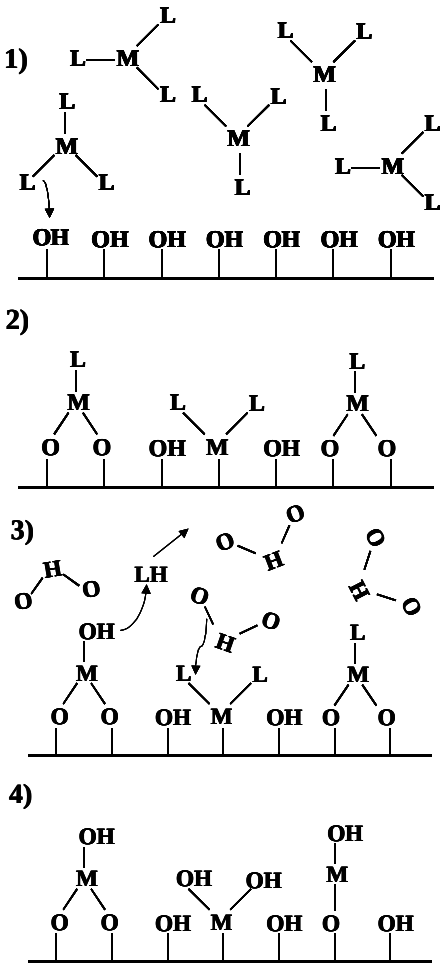

Figure 3. An imaginary ALD cycle for binary oxide film of metal (M) and oxygen (O). Precursors ML_3 (L = ligand, e.g. alkoxide) and H_2O are alternately pulsed. Between precursor pulses the reaction chamber is purged with inert gas.

In the case of ternary oxides the thin film is achieved simply by pulsing two metal oxides in different cycles. The metal ratio is then controlled by the ratio of the binary metal oxide cycles. In practice, designing the experiments and carrying out the depositions is not so straightforward. When ternary or more complex oxides are deposited by ALD, all constituent binary oxides must be deposited in a self-limiting manner at the same temperature. This requirement for similar deposition temperatures limits the number of possible precursors. Moreover, when binary oxides are combined

to produce multicomponent oxides, cations may behave differently because the surface chemistry differs from that in the binary processes.

Benefits of the ALD method relate mostly to the surface-controlled and self-limiting growth, which enable accurate control of thickness and conformal growth. Thickness is simply controlled by the number of cycles deposited. The same amount of thin film material is deposited during each cycle. ALD also enables excellent conformality and uniformity even in complicated three-dimensional structures.

3.2 ALD precursors

Precursor chemistry is an important issue in the development of new ALD processes. First of all, the precursors must be volatile and thermally stable both during vapor phase transport and on the growth surface. At their best, precursors chemisorb rapidly on the surface or react rapidly with the surface groups. This provides both effective use of the precursor and short pulse times. Precursors should also react completely to avoid impurities in the films.

Volatile metal precursors for ALD can be divided into five main categories: halides, *β*-diketonate complexes, alkoxides, true organometallics and amides.[42] For the preparation of oxide materials, the second precursor must be an oxide source. Depending on the metal precursor selected, the oxide source may be H_2O, H_2O_2, O_2, N_2O, or O_3. In the deposition of ternary and more complex oxides, the control of cation stoichiometry may be difficult. One way to control the stoichiometry is to use precursors that contain more than one of the desired film components. This kind of precursor contains two metal cations in the same ratio as in the desired film.[39] Another approach is to use an alkoxide together with a second metal-containing precursor. Here the alkoxide provides both metal and oxygen atom to the film.[43] The precursors used in the preparation of ternary and more complex films by ALD will now be discussed.

The characteristic feature of ALD is the self-limiting growth. This restricts the choice of precursors, and the single-source precursors which are successfully employed in CVD methods are not exploitable in ALD. The self-limiting growth mechanism is largely based on exchange reactions on the surface between alternately applied precursors. Thus, at least two precursors are required in an ALD process. Precursors also need to be stable against self-decomposition. Despite these requirements,

multicomponent oxide materials have successfully been deposited from a bimetallic precursor together with another metallic precursor and an oxidizing agent (see Table 1, p. 22). Besides bimetallic precursors, another types of precursors where a separate oxygen source is not needed will be discussed (see Table 2, p. 24).

A bimetallic precursor was recently utilized in ALD for the first time. $SrTa_2(OEt)_{10}(dmae)_2$ was used with O_2 plasma to deposit $SrTa_2O_6$.[44,45] $SrTa_2O_6$ has been widely studied due to its high permittivity and good thermal stability, but also because it is the core constituent of the more complex $SrBi_2Ta_2O_9$ (SBT) structure. SBT is mainly of interest for its use in ferroelectric random access memories. With the O_2 plasma process, a strontium-deficient composition was obtained with Sr to Ta ratio of only 0.27.[44] The carbon content in the as-deposited films was nevertheless low, being below the detection limit of Auger electron spectroscopy. Later, a less reactive oxygen source, H_2O, was used together with $SrTa_2(OEt)_{10}(dmae)_2$ as metal precursor.[46] With this combination, close to stoichiometric films were obtained with Sr to Ta ratio between 0.50 and 0.63 depending on the deposition temperature. Impurities were now clearly detectable, however. Carbon and nitrogen impurities were below 1%, but hydrogen impurities were typically between 1 and 3%. Growth rate was higher with the plasma-activated process. At 300 °C, growth rates were 0.8 and 0.23 Å/cycle for the O_2 plasma and water processes, respectively. Growth rate of the water process could be increased up to 0.33 Å/cycle with larger water dose.

A structurally related complex $SrTa_2(OEt)_{10}(ME)_2$, with methoxyethoxide ligand instead of dimethylaminoethoxide ligand, has also been studied (see Figure 4).[46,47] An ALD reaction with water produced relatively uniform films, though when the metal precursor was pulsed without an oxygen source the film thickness increased on the leading edge of the substrate indicating decomposition of the precursor.[46] Pulsing $SrTa_2(OEt)_{10}(ME)_2$ and O_2 plasma at 250 and 300 °C gave uniform and nearly stoichiometric films.[47] Saturative growth was demonstrated, and the films deposited at 250 °C were smooth with an rms roughness value of 0.23 nm as determined by atomic force microscopy (AFM). Carbon impurities were almost below the detection limit of X-ray photoelectron spectroscopy (XPS). In this case too, growth rate was higher with the plasma process than the water process: 0.5 Å/cycle, as against 0.3 Å/cycle at 250 °C.

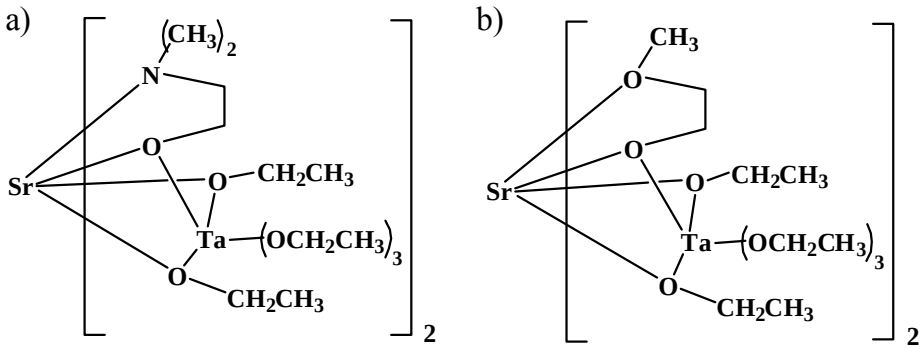

Figure 4. Two bimetallic precursors for strontium and tantalum: a) $SrTa_2(OEt)_{10}(dmae)_2$ (strontium bis(tantalum pentaethoxide dimethylamino-ethoxide)) b) $SrTa_2(OEt)_{10}(ME)_2$ (strontium bis(tantalum pentaethoxide methoxy-ethoxide)).

$SrTa_2(OEt)_{10}(dmae)_2$ and $SrTa_2(OEt)_{10}(ME)_2$ have also been used to prepare quaternary SBT. The bismuth precursors were $Bi(N(SiMe_3)_2)_3$ and $Bi(C_6H_5)_3$, respectively.[48,49] Slightly bismuth-rich and strontium-deficient SBT films were obtained with a pulsing ratio of two $Bi(N(SiMe_3)_2)_3/H_2O$ to one $SrTa_2(OEt)_{10}(dmae)_2/H_2O$.[48] Film growth rate was 0.28 Å/cycle. Impurity levels of carbon were moderate at 2-3 at.%. The hydrogen level was high in the as-deposited films, 19 ± 3 at.%, but was reduced to just 0.5 ± 0.1 at.% upon annealing. Time-of-flight elastic recoil detection analysis (TOF-ERDA) was used to determine the impurities.

In the case of the $SrTa_2(OEt)_{10}(ME)_2$ and $Bi(C_6H_5)_3$ process, precursors were dissolved together in *n*-butylacetate solvent and pulsed alternately with water.[49] A precursor mixing ratio of 1.0 was used in the solution. Films showed almost the same atomic ratio as with another precursor combination that was somewhat bismuth rich and strontium deficient. Carbon impurities were about 4 at.% as detected by Auger electron spectroscopy (AES).

Other precursors used in ALD besides compounds with strontium and tantalum are precursors with silicon and a metal (see Figure 5). The role of silicon is considered to be similar to that of a metal in the precursor and the resulting thin film material. Thus the term bimetallic is used for precursors that contain either two metals or metal and silicon. Precursors that contain silicon are typically used in the deposition of buffer

layers in the case of bismuth[50] and of high-*k* gate materials in the case of hafnium and lutetium[51-53].

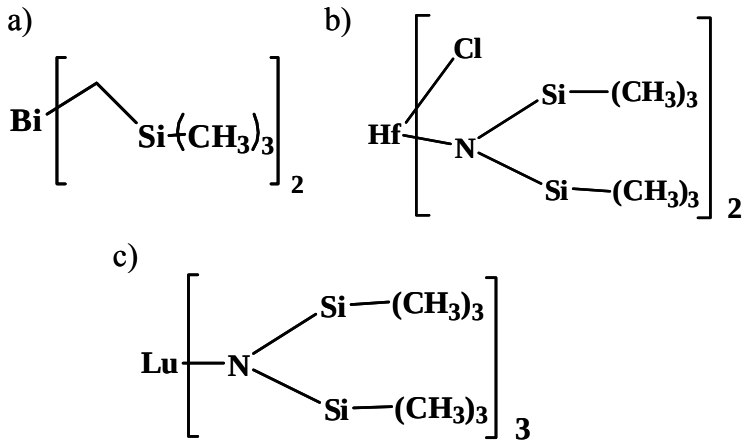

Figure 5. ALD bimetallic precursors containing metal and silicon: a) tris (trimethylsilylmethyl)bismuth ($Bi(CH_2SiMe_3)_3$ b) dichlorobis[bis(trimethylsilyl)-amido]hafnium $HfCl_2[N(SiMe_3)_2]_2$ c) tris[bis(trimethylsilyl)amido]lutetium $Lu[N(SiMe_3)_2]_3$.

Bismuth silicate was deposited using $Bi(CH_2SiMe_3)_3$ and ozone as precursors.[IV,V] Silicon to bismuth atomic ratio was found to increase from 1.5 to 4.5 with increasing deposition temperature. A constant growth rate of 0.4 Å/cycle was obtained between 250 and 350 °C. Increase of the bismuth content was achieved with use of an additional bismuth precursor, $BiPh_3$, at deposition temperature of 250 °C.[V] At this temperature it was possible to control the silicon to bismuth ratio within a range of 0.18 to 0.43. Detected by TOF-ERD analysis, impurity contents in the films were less than 0.2 at.% carbon and less than 0.1 at.% hydrogen.[IV]

In the case of hafnium silicate films, $HfCl_2[N(SiMe_3)_2]_2$ and H_2O were used as precursors and deposition temperatures from 150 to 400 °C were tested. [51] As with the bismuth silicate films, the silicon to metal ratio was found to increase with the deposition temperature. The increase in the silicon to hafnium ratio was linear from 0.18 to 0.43. Carbon, nitrogen, and chlorine impurities were below the detection limit, which was under 1 at.% for XPS. The highest growth rate, 1.3 Å/cycle, was obtained at deposition temperature of 250 °C. The growth rate increased up to 250 °C, but beyond

that it began to decrease. The hafnium silicate process with water was carefully studied by infrared (IR) spectroscopy.[52] First, the IR studies established that the change in the growth rate was related to hydroxyl group saturation, which remained constant before decreasing above 250 °C. Secondly, they revealed that enhanced ligand dissociation and reaction of the functional groups ($Si\text{-}(CH_3)_x$) with water when the deposition temperature is increased leads to increased silicon incorporation in the film. An analogous precursor combination has been used for zirconium, viz. $ZrCl_2[N(SiMe_3)_2]_2$.[54] However, silicon incorporation was much lower in this case. A maximum silicon to zirconium ratio of 0.22 was obtained at deposition temperature of 350 °C. After annealing, the films contained crystalline ZrO_2 rather than silicate phase.

Lutetium silicate films have been deposited with use of $Lu[N(SiMe_3)_2]_3$ as a precursor for Lu and Si.[53] Two different oxidizing agents were tested: H_2O and O_3. At deposition temperature of 380 °C, the silicon to lutetium atomic ratio was 1.1 with H_2O and 1.5 with O_3. XPS data showed that the films were lutetium silicate rather than a mixture of silicon oxide and lutetium oxide.

Table 1. ALD processes where bimetallic precursors have been employed.

Thin film material	Metal precursors	Oxygen source	Metal ratio	Deposition temperature °C	Ref.
$SrTa_2O_6$	$SrTa_2(OEt)_{10}(dmae)_2$	O_2 plasma	Sr/Ta 0.27	300	44
	$SrTa_2(OEt)_{10}(dmae)_2$	O_2 plasma	not given	200	45
	$SrTa_2(OEt)_{10}(dmae)_2$	H_2O	Sr/Ta 0.50-0.63	200-350	46
	$SrTa_2(OEt)_{10}(ME)_2$	O_2 plasma	Sr/Ta 0.43-0.6	250-300	47
	$SrTa_2(OEt)_{10}(ME)_2$	H_2O	not given	200-350	46
$SrBi_2Ta_2O_9$	$SrTa_2(OEt)_{10}(ME)_2$ + $BiPh_3$	O_2 plasma	Sr/Ta 0.45 Bi/Ta 1.1	250	49
	$SrTa_2(OEt)_{10}(dmae)_2$ + $Bi(N(SiMe_3)_2)_3$	H_2O	Sr/Ta 0.4 Bi/Ta 1.05	190	48
Bi_2SiO_5	$Bi(CH_2SiMe_3)_3$	O_3	Si/Bi 1.5-4.8	200-450	IV
	$Bi(CH_2SiMe_3)_3$ + $BiPh_3$	O_3	Si/Bi 0.12-1.9	250	V
Hf-Si-O	$HfCl_2[N(SiMe_3)_2]_2$	H_2O	Si/Hf 0.18-0.43	150-400	51,52
Lu-Si-O	$[(Me_3Si)_2N]_3Lu$	H_2O	1.1	380	53
		O_3	1.5		

An obvious difficulty in ALD is the deposition of metal oxide directly onto pure silicon substrate. Silicon is easily oxidized, with the formation of interfacial silicon dioxide. Thin films are deposited layer by layer in ALD. However, a single layer rarely covers the entire substrate surface due to precursor size or other limiting factors. Because of this, the oxidizing precursor pulse after the first metal precursor pulse will easily diffuse and oxidize the underlying silicon substrate. An interfacial silicon dioxide layer is likely to affect the performance of an integrated circuit based on silicon.[55] Use of two different metal precursors without a separate oxide source has been proposed as a novel way to avoid oxidation of the silicon substrate.[43,56-61] Such precursors also provide three

different constituents of the thin film material from just two precursors (see Table 2, p. 24). A common combination has been metal chloride together with a metal alkoxide where the alkoxide provides oxygen to the film. This kind of approach was introduced by Ritala *et al.*,[43] who studied a variety of precursors with promising results. Even though the metal ratio in ternary oxide films did not correspond to the ratio expected, the films were grown in a self-limited manner, and films were uniform with sharp silicon-metal oxide interfaces. Another important result was the incorporation of silicon into the oxide phase, which has not been easy to achieve by ALD. Silicon was uniformly incorporated into Zr-Si-O films, and the precursor for silicon was either silicon ethoxide or silicon butoxide.

Overall, impurities in the studies of Ritala *et al.*[43] were less than 1 at.% for carbon and hydrogen and 0.8-2.0 at.% for chlorine. An exception to this general behavior was the $AlCl_3/Ti(O^iPr)_4$ process at 300 °C and the $ZrCl_4/Si(O^nBu)_4$ at 250 °C, which left chlorine residues of 4.0 and 8.3 at.%, respectively. Later study was made of similar chloride/alkoxide processes of zirconium and hafnium silicates.[57,58,61] In these processes both the composition ratio [M/(M+Si)] and impurity contents decreased with increasing deposition temperature. The same result was obtained for the $ZrCl_4/Si(O^nBu)_4$ process.[43]

A further example of the alkoxide-based processes is the use of metal nitrate, such as $Hf(NO_3)_4$, as a source of metal and oxygen. Ternary oxides were deposited by introducing either $AlCl_3$ or $ZrCl_4$ as a second precursor.[59] Another approach to the chloride and alkoxide precursor combination is to use metal alkyl amide instead of metal chloride, and *t*-butoxy silanol instead of metal alkoxide.[60] The $Hf(N(CH_3)_2)_4$ and $(^tBuO)_3SiOH$ precursor combination resulted in hafnium silicate glass films corresponding to the stoichiometry of $HfO_2(SiO_2)_x$. Depending on the deposition conditions, the metal ratio varied between x=2 and 3. While chlorine residues were avoided, nitrogen impurities were introduced. However, according to RBS, nitrogen and carbon impurities were both less than 2 at.%. TEM revealed that also with this type of precursor, the interfacial oxide could be reduced below 1 nm.

Table 2. ALD processes where ternary films have been made without a separate oxide source.

Thin film material M_1-M_2-O	Metal precursor	Alkoxide or other oxygen-containing precursor	Metal ratio $M_1/(M_1+M_2)$	Deposition temperature °C	Ref.
Al-Ti-O	$AlCl_3$	$Ti(O^iPr)_4$	0.8	300	43
Zr-Al-O	$ZrCl_4$	$Al(OEt)_3$	0.28	400	43
Zr-Ti-O	$ZrCl_4$	$Ti(O^iPr)_4$	0.45	300	43
Zr-Si-O	$ZrCl_4$	$Si(OEt)_4$	0.39	500	43
	$ZrCl_4$	$Si(O^nBu)_4$	0.53, 0.30	250,500	43
	$ZrCl_4$	$Si(O^nBu)_4$	0.40-0.23	300-500	57
	$SiCl_4$	$Zr(O^tBu)_4$	0.75-0.53	125-225	58
Hf-Al-O	$HfCl_4$	$Al(OEt)_3$	0.33	400	43
	$AlCl_3$	$Hf(NO_3)_4$	Not given	150-190	59
Hf-Ti-O	$HfCl_4$	$Ti(O^iPr)_4$	0.24	300	43
Hf-Si-O	$Hf(N(CH_3)_2)_4$	$(^tBuO)_3SiOH$	0.25-0.33	250-350	60
	$HfCl_4$	$Si(O^nBu)_4$	0.46-0.19	250-500	61
Hf-Zr-O	$ZrCl_4$	$Hf(NO_3)_4$	Not given	150-190	59

3.3 Deposition of Pb and Bi compound films by ALD

Deposition of lead and bismuth oxide films by ALD is challenging because of the scarcity of good precursors. A survey of the few reported studies on lead and bismuth based oxides is presented below.

3.3.1 Lead-containing materials

Although PZT is one of the most frequently studied materials for FeRAM[16] devices, there are relatively few ALD processes for lead-containing thin films (Table 3). However, the continuous scaling down of microelectronic devices will soon require deposition methods with better step coverage – methods such as ALD. The growth of PZT and other related lead-containing oxides has been widely studied by physical methods and by chemical methods apart from ALD. Lack of a good binary process for lead oxide is the major problem in ALD, but another challenge is to find a good combination of precursors for Zr and Ti – precursors that can be deposited at similar

temperatures and with similar growth rates to the lead oxide precursor. Safety issues must also be addressed. Lead is an environmentally hazardous element and finding lead-free alternatives would be desirable. For the moment, PZT has several superior properties that argue against its replacement. These include higher switching charge per area and lower deposition temperature and post-deposition annealing temperature than other materials that have been tested.[16,62] In this context, it should be noted that, currently, the processes producing nanometer-scale thin films of lead-based oxides represent a much less severe environmental problem than soldering processes in the electronics industry, which are still mainly based on lead and its alloys.

Lead sulfide was the first lead compound to be processed by ALD. Interest in PbS stems from its photoconduction properties, especially its high response in the near infrared, which gives it use as sensor material. In the first study, five different lead precursors were explored, namely $PbBr_2$, PbI_2, $(CH_3COO)Pb$, $Pb(thd)_2$, and $Pb(dedtc)_2$.[63] Since the first three yielded very slow growth rates, only the last two were studied in detail. Later, two lead tert-butoxide complexes, $[Pb(O^tBu)_2]_2$ and $Pb_4O(O^tBu)_6$, were investigated.[64] The sulfur source in all experiments was H_2S. Films deposited from $Pb(dedtc)_2$ were found to be p-type semiconductors with hole mobility and concentration similar to those observed in previously studied chemically deposited films.[63] PbS films deposited on glass and on polycrystalline alumina had relatively rough surfaces according to scanning electron microscopy (SEM).[63]

Lead has also been used as a dopant in CaS and SrS thin films deposited by ALD.[65-70] The main goal in doping CaS and SrS matrices with Pb^{2+} ions was to produce blue light in color electroluminescence (EL) devices. The Pb^{2+} ion has s^2 outer electron configuration, and its luminescence properties are thus highly dependent on the matrix environment. Although previous studies had identified some differences between CaS and SrS matrices, the doping with lead precursors was more carefully studied than the matrices. It appears that the blue emission originates from dimers formed by Pb^{2+} ions.[69] For selective doping, therefore, it is important to employ dimers rather than single atoms or larger aggregates. In tests of four different precursors, namely $PbCl_2$, $PbBr_2$, $Pb(thd)_2$, and $Pb(dedtc)_2$, $Pb(dedtc)_2$ gave the most homogeneous doping at the deposition temperature chosen, viz. 450 °C.[65] The most intense blue emission was achieved with Pb concentration in the range of 1.0-1.5 mol.%. L_{25} brightness values for

CaS:Pb and SrS:Pb were 2.5 and 17 cd/m^2, respectively, at 300 Hz. Much higher luminance values for CaS:Pb samples were obtained when $PbEt_4$ rather than $Pb(dedtc)_2$ was used as lead precursor.[66] The L_{25} value was higher than 80 cd/m^2 at 60 Hz for samples containing 0.6-2.5 mol.% of lead. These much higher values were attributed to the low deposition rate. If the deposition rate is much lower than one monolayer per cycle, the formation of larger aggregates is likely to be diminished. Also, the deposition temperature plays a role. Even though annealing temperatures were higher than in previous studies (725 °C), very low luminance values were obtained with $Pb(C_5{}^tBu_3H_2)_2$ as precursor.[70] It was assumed that the main reason for lower luminance values was actually the low deposition temperature. When films were deposited at 280 °C the best emitting value was only 6 cd/m^2. In another study of the effect of deposition temperature, increasing the deposition temperature from 350 to 400 °C improved the blue emission of CaS:Pb devices.[69]

Lead oxide processes have been studied by ALD mainly to deposit the more complex lead titanate $PbTiO_3$. For lead oxide depositions only four different precursors have been studied so far: Ph_4Pb[I], $Pb(thd)_2$[I], $Pb(tmod)_2$[71], and $Pb(OCMe_2CH_2NMe_2)_2$[72]. In these studies, the oxidizing agent for Ph_4Pb and $Pb(thd)_2$ was ozone, while that for $Pb(tmod)_2$ and $Pb(OCMe_2CH_2NMe_2)_2$ was water. Even though no actual ALD window was observed for Ph_4Pb/O_3 and $Pb(thd)_2/O_3$ processes, self-limiting growth was confirmed at the temperatures studied, 250/300 °C and 150 °C, respectively. Growth rate for the Ph_4Pb/O_3 process was 0.13 Å/cycle at 250 °C. For the $Pb(thd)_2/O_3$ process, a much higher growth rate of 1.0 Å/cycle was observed at 150 °C. For $Pb(tmod)_2$, self-limiting growth was observed at 240 and 300 °C even though the films were not uniform in thickness.[71] In the case of $Pb(OCMe_2CH_2NMe_2)_2$, an ALD window was observed between 190 and 280 °C when the temperature region 150-325 °C was explored. Growth rate inside the ALD window was 0.2 Å/cycle. However, the reported purge times were high, being 40 s and 15 s after the Pb precursor and H_2O pulses, respectively.[72] Maximum pulse and purge times in other reported lead oxide processes have not exceeded 2 s.[I,71]

The first ALD process for lead titanate was recently published[II] as part of this thesis and will be discussed in more detail in Chapter 4. The precursors were Ph_4Pb/O_3 and $Ti(O\text{-}i\text{-}Pr)_4/H_2O$. Careful optimization of the precursor pulsing ratio resulted in

stoichiometric $PbTiO_3$ at the two temperatures studied (250 and 300 °C). The as-deposited films were amorphous and annealing was necessary to obtain the crystalline perovskite phase. Impurity contents of the films were low: below 0.2% for carbon and below 0.5% for hydrogen. Roughness values (rms values), determined by AFM, were unexpectedly high compare to the rather low rms values of the binary oxides.[I,73] An rms-value of 23.8 nm was obtained for 210-nm-thick lead titanate film. An interesting result was that the growth rate of the lead titanate film as compared with the growth rate calculated from the rates for the binary oxides was 55% higher at the deposition temperature of 250 °C. The highest growth rate was obtained when the lead to titanium atomic ratio in the films was 1.7. The rate was decreased when the relative amount of lead in the film was decreased. Evidently the different reactivity of the precursors with the already deposited Pb-O or Ti-O layer was responsible for the changes in the relative growth rate.

Quite similar results were recently obtained by Hwang *et al.*[72] when they used $Pb(OCMe_2CH_2NMe_2)_2$ (see Figure 6) and $Ti(O^tBu)_4$ as metal precursors and water as oxidant. As a substrate they used $Ir/IrO_2/SiO_2/Si$ electrodes. They found the growth rate of lead titanate to increase whit increase in the relative amount of lead in the films. When stoichiometric lead titanate films were deposited, the growth rate was four times the rate calculated from the growth rates of the constituent oxides. Hwang *et al.*[72] suggested that the catalytic nature of titanium dioxide was the reason for this increase. They also proposed that, in this lead titanate process, there is a certain incubation period during the early stages of the thin film growth. When they deposited films of different thickness, the results for films below 10 nm were quite different from the results for thicker films, which were close to stoichiometric. First, the growth rate was higher for the thinner than the thicker films. Secondly, the thin films were lead-rich compared to the composition of the thicker films having close to the stoichiometric atomic ratio. Beyond a thickness of about 10 nm, both growth rate and atomic ratio were constant. Hwang *et al.*[72] believe that, during the initial stage, Pb precursors more easily adsorb on to the substrate surface and, therefore, Pb excess in the films leads to faster growth rate. After rapid thermal annealing, the stoichiometric films crystallized in perovskite structure. Impurities were analyzed by AES, and carbon content of the films was below 1%. Also the roughness values were extremely low rms-value being

below 1.1 nm as analyzed by AFM. The dielectric constant was 280 and the remnant polarization was 11.2 μC/cm^2 at an applied bias voltage of 2.8 V.

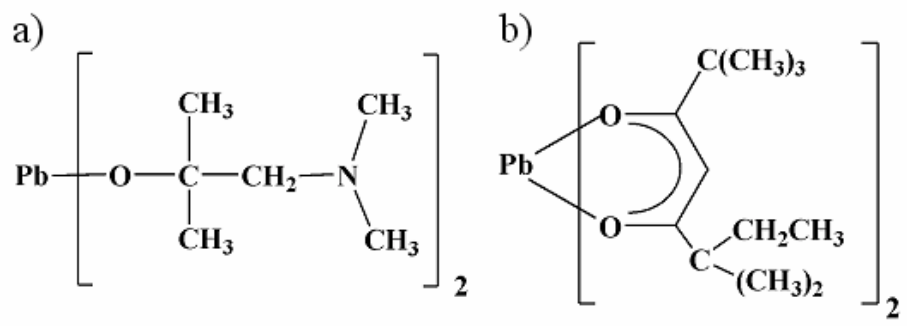

Figure 6. Lead precursors used in depositions of lead titanate by ALD: a) bis(3-N,N-dimethyl-2-methyl-2-propanoxide) $Pb(OCMe_2CH_2NMe_2)_2$ and b) bis(2,2,6,6,-tetramethyl-3,5-octanedionato)lead $Pb(tmod)_2$.

Watanabe *et al.*[71] used $Pb(tmod)_2$ (see Figure 6) and $Ti(O\text{-}i\text{-}Pr)_2(thd)_2$ precursors for lead and titanium, respectively. Precursors were dissolved in ethylcyclohexane and injected separately to the reaction chamber. Water was used as oxidant. Pb-Ti-O films were deposited at 240 and 300 °C. Stoichiometric lead titanate was obtained by combining lead and titanium oxide processes in the ratio of 1:4 or 1:6. Even though saturative growth was observed for both binary oxide processes, the ternary Pb-Ti-O process was nonsaturative. Increasing the lead precursor injection linearly increased both the atomic ratio and the growth rate. Watanabe *et al.*[71] suspected that this was caused by the Ti-O layer, which either catalyzed the decomposition of the Pb precursor or enhanced its oligomerization. Later, a different lead precursor, $Pb(thd)_2$, was introduced together with $Ti(O\text{-}i\text{-}Pr)_2(thd)_2$.[74] Also in this experiment, precursors were dissolved in ethylcyclohexane and injected seperately to the reaction chamber. Close to stoichiometric films were obtained with lead to titanium pulsing ratio of 1:8 at deposition temperature of 240 °C. Again the process was not ideally self-regulated. However, depositions on a three-dimensional substrate with deep holes gave promising results. Cation distribution was much better than in previous CVD studies of lead titanate. In both processes,[71,74] as-deposited films were amorphous, and impurity contents of carbon were 2% as detected by XPS.

A lead zirconate process is the most recently introduced ALD process for lead and will be discussed in more detail in Chapter 4. In this process, Ph_4Pb and $Zr(thd)_4$ were used as precursors together with ozone.[III] The process was studied at 250 and 300 °C and the atomic ratio of the thin films was controlled by changing the pulsing ratios of the constituent oxides. The crystalline perovskite phase was observed after annealing of the thin film deposited on a single crystalline $SrTiO_3$ substrate.

It is worth noting that in all ternary lead oxides an excess of lead in the thin films was desirable as it either enhanced the crystallinity[II,III] or promoted the preferred orientation of the films.[72]

Table 3. Lead-containing films deposited by ALD.

Thin film material	Metal precursors	Non-metallic source	Deposition temperature, °C	Ref.
PbS	$PbBr_2$	H_2S	300-350	63
	PbI_2			
	$Pb(CH_3COO)_2$			
	$Pb(thd)_2$			
	$Pb(dedtc)_2$			
PbS	$[Pb(O^tBu)_2]_2$	H_2S	130-390	64
	$Pb_4O(O^tBu)_6$		130-390	
	$Pb(thd)_2$		130-390	
	$Pb(dedtc)_2$		220-340	
Dopant in SrS and CaS	$PbCl_2$	H_2S	450	65
	$PbBr_2$			
	$Pb(thd)_2$			
	$Pb(dedtc)_2$			
Dopant in CaS	$PbEt_4$	H_2S	390	66-68
			350-400	69
Dopant in SrS	$Pb(C_5{}^tBu_3H_2)_2$	-	280	70
PbO_2	Ph_4Pb	O_3	185-400	I
	$Pb(thd)_2$	O_3	150-300	
	$Pb(dedtc)_2$	O_3	300-350	
$PbTiO_3$	Ph_4Pb + $Ti(O\text{-}i\text{-}Pr)_4$	O_3	250, 300	II
		H_2O		
	$Pb(tmod)_2$ +	H_2O	240, 300	71
	$Ti(O\text{-}i\text{-}Pr)_2(thd)_2$			
	$Pb(OCMe_2CH_2NMe_2)_2$+	H_2O	200	72
	$Ti(O^tBu)_4$			
	$Pb(thd)_2$ +	H_2O	240	74
	$Ti(O\text{-}i\text{-}Pr)_2(thd)_2$			
$PbZrO_3$	Ph_4Pb + $Zr(thd)_4$	O_3	250, 300	III

3.3.2 Bismuth-containing materials

Bismuth-containing oxides show promise for applications in several fields of technology. $Bi_2Ti_2O_7$ and amorphous Bi-Ti-Si-O are dielectric materials and could be exploited for capacitor dielectrics in dynamic random access memories (DRAMs).[75,76] $Bi_4Ti_3O_{12}$ and SBT, in turn, are ferroelectric materials and have been actively studied as potential materials for FeRAMs. These materials and other bismuth oxides have been studied by ALD (Table 4) and are reviewed in the following.

Bismuth oxide depositions by ALD have not been completely successful. With $Bi(N(SiMe_3)_2)_3$ and H_2O as precursors, BiO_x films were deposited in a narrow temperature range of 190-200 °C.[48] Film growth was not reproducible, however, probably because of the partial reduction of bismuth to its metallic form. Attempts to use $BiPh_3$ as metal precursor, and H_2O_2[77] as well as O_3[V] as oxidant, failed to produce bismuth oxide. $BiCl_3$ together with water resulted in BiOCl formation.[78]

While the production of binary bismuth oxide by ALD has not been successful, the addition of the titanium dioxide process to produce bismuth titanate has given promising results. The bismuth precursors used in these processes have been $BiPh_3$ oxidized by H_2O[77] or O_3,[V] $Bi(N(SiMe_3)_2)_3$ oxidized with H_2O,[21] and $Bi(mmp)_3$ oxidized with O_2/O_3 mixture[79] or H_2O[75] (see also Figure 7).

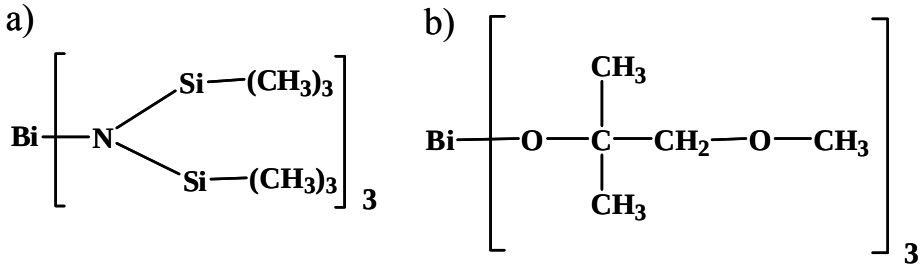

Figure 7. Bismuth precursors used in depositions of bismuth titanate by ALD: a) tris[bis(trimethylsilyl)amide], $Bi(N(SiMe_3)_2)_3$ and b) tris(1-methoxy-2-methyl-2-propoxy)bismuth, $Bi(mmp)_3$.

In the first Bi-Ti-O study,[77] $BiPh_3$ and H_2O were used as precursors and 260 °C as the growth temperature. Uniform films were achieved, but the Bi/Ti metal ratio never

exceeded 0.61 whatever the pulsing ratio. Higher Bi/Ti metal ratios were achieved when ozone instead of water was used as the oxidant to react with $BiPh_3$ at the deposition temperature of 250 °C.[V] Titanium isopropoxide and water were used in both processes as sources for titanium dioxide.

When water was used as oxidant for $BiPh_3$[77] and for $Bi(mmp)_3$[75] in the deposition of bismuth titanate films, metallic bismuth was observed in the as-deposited films. In the case of the $BiPh_3/H_2O;Ti(O\text{-}i\text{-}Pr)_4/H_2O$ process, metallic bismuth was observed by X-ray diffraction (XRD) when the Bi/Ti atomic ratio exceeded 0.35 at the deposition temperature of 260 °C. In the $Bi(mmp)_3/H_2O;Ti(mmp)_3/H_2O$ process, metallic bismuth was deposited above 275 °C when 1:1 metal pulsing ratio was used. Although metallic bismuth was present when the $Bi(N(SiMe_3)_2)_3/H_2O$ process was used to produce the binary oxide, no metallic bismuth was observed when the $Ti(OMe)/H_2O$ process was added to produce ternary Bi-Ti-O thin films.[21,48] When a stronger oxidizing agent like O_3 was used, no metallic form of bismuth was observed under any conditions.[79,V]

Neither $Bi_2Ti_2O_7$[75,77,V] nor $Bi_4Ti_3O_{12}$[21,79,V] was crystallized regardless of the bismuth content in the as-deposited films. Bismuth titanate crystallized after annealing at 700-800 °C. Vehkamäki *et al.*[21] found that crystallization of $Bi_4Ti_3O_{12}$ was initiated at 500 °C; the orientation was random below 650 °C, but c-axis orientation, together with some minor orientations was found at 750 °C.

Electrical measurements on ALD bismuth titanate films showed films with lower bismuth content, viz. $Bi_2Ti_2O_7$ thin films, to have relative permittivity of about 45-60.[77,75] In studies of ferroelectric properties of films richer in Bi, i.e. $Bi_4Ti_3O_{12}$, Vehkamäki *et al.*[21] found that c-axis oriented films had inferior electrical properties to randomly oriented films. When capacitors with a 51-nm-thick $Bi_4Ti_3O_{12}$ ferroelectric film were preannealed for 10 min at 500 °C and then annealed for 60 min at 600 °C, the permittivity increased to 160 with a remnant polarization of 0.5 $\mu C/cm^2$. Even higher permittivity values for $Bi_4Ti_3O_{12}$ thin films were obtained by Cho *et al.*[79] They used ALD in injection mode with mixed $Bi(mmp)_3$ and $Ti(mmp)_3$ precursors in ethyl cyclohexane solution together with O_2/O_3 oxidizing mixture. Stoichiometric films were obtained by adjusting the mixing ratio of the Bi/Ti solution. However, no proof of self-limiting ALD growth was obtained.

Deposition of Bi_2SiO_5 by exploiting the $Bi(CH_2SiMe_3)_3/O_3$ process is another example of using bimetallic precursors to produce ternary thin films.[IV] The $Bi(CH_2SiMe_3)_3/O_3$ process was modified by adding the $BiPh_3/O_3$ process to increase the bismuth content in the thin films.[V] These two processes will be discussed in more detail in Chapter 4.

The growth of more complex bismuth oxides by ALD has also been demonstrated. Vehkamäki *et al.*[48] first demonstrated Bi-Ta-O film growth using the $Bi(N(SiMe_3)_2)_3/H_2O;Ta(OEt)_5/H_2O$ process at 190 °C. Self-limiting growth with a 0.3 Å/cycle deposition rate was confirmed. Similarly, they deposited Sr-Bi-Ta-O (SBT) films with use of bimetallic $SrTa_2(OEt)_{10}(dmae)_2$ and $Bi(N(SiMe_3)_2)_3$ as precursors and 2:1 pulsing ratio (Sr/Bi).[48] A similar process but with plasma enhancement to produce SBT was demonstrated by Shin *et al.*[47] Bimetallic $SrTa_2(OEt)_{10}(ME)_2$ and $BiPh_3$ were used to form the precursor solution, which was injected into the ALD chamber at 250-300 °C. In the studies of both groups, the films were slightly strontium deficient. The as-deposited films were amorphous and the preferred polycrystalline ferroelectric phase was observed only after annealing above 750 °C. Vehkamäki *et al.*[48] were able to improve the phase purity by depositing a 30-nm-thick crystalline film as seed layer before further depositing a 170-nm film.

Another attempt to grow a complex bismuth compound by ALD involved the Bi-Ti-Si-O phase.[76,80,81] The precursor was a solution of $Bi(mmp)_3$, $Ti(mmp)_4$, $Si(OEt)_4$ dissolved in ethylcyclohexane with either O_3[80,76] or H_2O[81] as oxidant. The observed growth rate was similar with the two oxidants, being about 0.21 Å/cycle. An ALD window was observed between 200 and 350 °C in the process oxidized by water. The cation Bi/Ti/Si stoichiometry was 0.38/0.37/0.25 with the ozone process and 0.28/0.59/0.13 with the water process at 300 °C. The obtained films were amorphous after the deposition, and crystallization commenced at 480 °C. The dielectric constant was between 24 and 64 depending on the cation stoichiometry.

Slight modification to Bi-Ti-Si-O thin films was made by Min *et al.*[82] who replace silicon with aluminum to produce Bi-Ti-Al-O thin films. A solution of $Bi(mmp)_3$ and $Ti(mmp)_3$ dissolved in ethylcyclohexane was used as precursors together with

trimethylaluminum (TMA) and H_2O as a oxidant. Dielectric constant decreased while the insulating properties were improved with the increasing aluminum content.

Table 4. Bismuth-containing oxide films deposited by ALD.

Thin film material	Metal precursors	Oxygen source	Deposition temperature, °C	Ref.
BiO_x	$Bi(N(SiMe_3)_2)_3$	H_2O	190-200	48
Bi-Ti-O	$BiPh_3$,	O_3	250	V
	$Ti(O\text{-}i\text{-}Pr)_4$	H_2O		
	$BiPh_3$, $Ti(O\text{-}i\text{-}Pr)_4$	H_2O	260	77
	$Bi(mmp)_3$, $Ti(O\text{-}i\text{-}Pr)_4$	H_2O	225-300	75
	$Bi(N(SiMe_3)_2)_3$, $Ti(OMe)_4$	H_2O	190	21
	$Bi(mmp)_3$, $Ti(mmp)_4$	O_2/O_3	250-500	79
Bi_2SiO_5	$Bi(CH_2SiMe_3)_3$	O_3	200-450	IV,V
	$Bi(CH_2SiMe_3)_3$, $BiPh_3$	O_3	250	V
Bi-Ta-O	$Bi(N(SiMe_3)_2)_3$, $Ta(OEt)_5$	H_2O	190	48
Sr-Bi-Ta-O	$Bi(N(SiMe_3)_2)_3$,	H_2O	190	48
	$SrTa_2(OEt)_{10}(dmae)_2$			
	$BiPh_3$,$SrTa_2(OEt)_{10}(ME)_2$	O_2 plasma	250	49
Bi-Ti-Si-O	$Bi(mmp)_3$,$Ti(mmp)_4$,$Si(OEt)_4$	O_3	300	80
		O_3	200-375	76
		H_2O	200-450	81
Bi-Ti-Al-O	$Bi(mmp)_3$,$Ti(mmp)_4$, TMA	H_2O	250	82

4 Experimental

This section summarizes the materials, instruments, and methods used in this the work. More detailed descriptions of the depositions and characterizations can be found in publications I-V.

4.1 Precursors and substrates

Metal precursors. For the lead oxide experiments the metal precursors were lead diethyl dithiocarbamate ($Pb(dedtc)_2$), lead 2,2,6,6-tetramethyl-3,5-heptanedione ($Pb(thd)_2$), and tetraphenyl-lead (Ph_4Pb). In the ternary lead oxide experiments, the lead precursor was Ph_4Pb. Synthesis of $Pb(dedtc)_2$ and $Pb(thd)_2$ was done by methods described in the literature[83,84] and purification was done by sublimation. Commercial Ph_4Pb (97%) was purchased either from Aldrich Chemical Co., Milwauke, USA, or Acros Organics, New Jersey, USA. The stability and volatility of the lead precursors were evaluated by thermogravimetry (TG).

Ternary bismuth oxides were deposited from two different metal precursors. Tris(trimethylsilylmethyl)bismuth ($Bi(CH_2SiMe_3)_3$) was used as a bimetallic precursor for the Bi-Si-O thin film depositions. Triphenyl bismuth $BiPh_3$ was used both to enhance the bismuth content in Bi-Si-O thin films and to deposit Bi-Ti-O thin films. $Bi(CH_2SiMe_3)_3$ was synthesized and characterized by Timo Hatanpää at the University of Helsinki.[II] $BiPh_3$ (99%) was purchased from Strem Chemicals, Newburyport, USA.

Titanium isopropoxide $Ti(O\text{-}i\text{-}Pr)_4$ (Aldrich Chem. Co., 97%) was used as titanium precursor for the lead titanate and bismuth titanate experiments. Previous ALD studies of TiO_2 involving the $Ti(O\text{-}i\text{-}Pr)_4/H_2O$ process were used to optimize the parameters for the ternary oxide experiments.[73] The zirconium precursor for lead zirconate depositions was zirconium 2,2,6,6-tetramethyl-3,5-heptanedione ($Zr(thd)_2$). This was either commercial (Strem Chemicals, 99%, Newburyport, USA) or synthesized.[85] A previously reported[86] ALD process for producing ZrO_2 from $Zr(thd)_2/O_3$ was used as the starting point when lead zirconate deposition parameters were optimized.

Examples of different types of precursors used in this study are schematically presented in Figure 6.

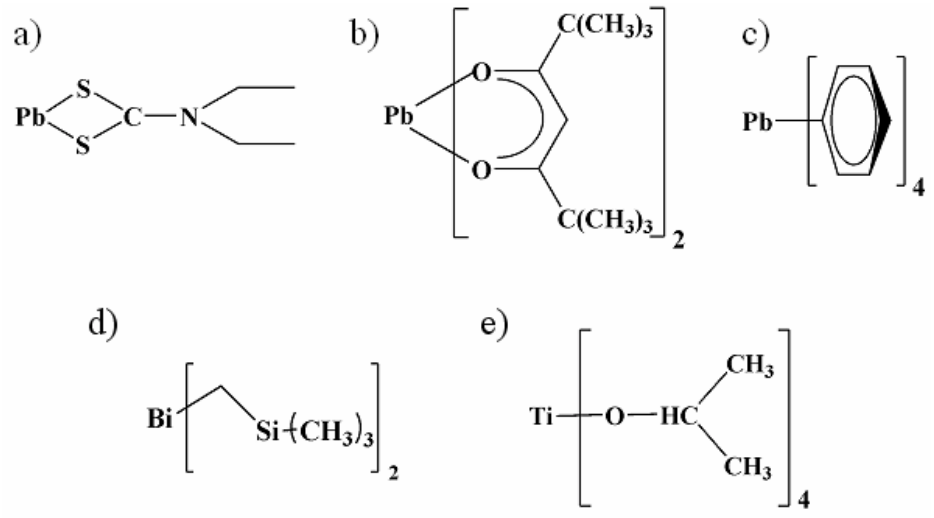

Figure 6. Examples of different types of precursors used in this study: a) lead diethyl dithiocarbamate ($Pb(dedtc)_2$), b) lead 2,2,6,6-tetramethyl-3,5-heptanedione ($Pb(thd)_2$), c) tetraphenyl-lead (Ph_4Pb), d) tris(trimethylsilylmethyl)bismuth ($Bi(CH_2SiMe_3)_3$), e) titanium isopropoxide Ti(O-*i*-Pr)$_4$.

Oxygen precursors. Either ozone or water was used as the oxygen source. Ozone was used with all lead- and bismuth-containing metal precursors as well with the zirconium precursors. Water was only used to oxidize the titanium precursors, titanium isopropoxide Ti(O-*i*-Pr)$_4$. Ozone was generated from oxygen (>99.999%) in an ozone generator (Fischer model 502). Ozone concentration was confirmed by iodometric titration and found to be approximately 4%.[87] Water was vaporized and introduced into the reactor space from an external cylinder kept at room temperature.

Carrier and purge gases. Nitrogen served as carrier and purge gas in all experiments. High purity (>99.999%) nitrogen (N_2) gas was produced from air in a Nitrox UHPN 3000-1 nitrogen generator.

Substrates. Most experiments were done on Si(100) silicon wafers. Wafers were used without cleaning and thus were covered by native oxide. Bismuth silicate films were also deposited on titanium foil (99.6%) in order to study the bismuth and silicon contents by XRF. In addition, crystallinity and diffusion behavior of bismuth silicate were studied on sapphire (single crystalline Al_2O_3) and on Si(100) buffered with

MgO,[88] ZrO_2,[86] or YSZ[89] (yttrium-stabilized zirconium oxide). $SrTiO_3$(100) substrates were used together with Si(100) and MgO-buffered Si(100) to study the growth of $PbZrO_3$.

4.2 Deposition of Pb and Bi oxide thin films

New ALD processes were developed for lead oxide, lead titanate, lead zirconate, and bismuth silicate. A new and stronger oxidizing agent, O_3, as distinct from previously used water[77] was used for $BiPh_3$ oxidation when bismuth titanate was deposited.

Thin film depositions were carried out in a commercial hot-wall flow-type ALD reactor (F-120) manufactured by ASM Microchemistry Ltd. Pressure inside the reactor during depositions was 2-3 mbar. The metal precursors were evaporated inside the reactor from open glass boats. Sublimation/evaporation temperatures and pulsing times for the metal precursors are listed in Table 5. Purge times were between 1 and 2 s depending on the precursor pulsed immediately before the purge. Ozone pulse duration was between 1 and 2 s depending on the metal precursor pulsed before ozone. The water pulse was kept constant at 1 s. Deposition temperatures for binary oxide processes and the bismuth silicate processes are presented in Table 5. Deposition temperatures for other ternary oxides were 250 and 300 °C for lead titanate, 275 and 300 °C for lead zirconate, and for bismuth titanate 250 °C.

Table 5. Precursors, sublimation/evaporation temperatures and pulse times used in the ALD studies of this work.

Metal precursor	Sublimation/evaporation temperature, °C	Deposition temperature, °C	Precursor pulsing time, s
$Pb(dedtc)_2$	190	300-350	1
$Pb(thd)_2$	110-115	150-300	2
Ph_4Pb	160-170	185-400	1.5
$Bi(CH_2SiMe_3)_3$	45	200-450	1
$BiPh_3$	115		1
$Ti(O\text{-}i\text{-}Pr)_4$	40 (liquid)		0.6
$Zr(thd)_4$	130		1

In the case of ternary films, post-deposition annealing was used to enhance crystallization. Samples were annealed in a rapid thermal annealing (RTA) oven (PEO 601, ATV Technologie GmbH) in either N_2 or O_2 atmosphere. In the case of bismuth titanate films, tube furnace heating in air was used as well.

4.3 Film characterization

Profilometry was used to measure thicknesses of poorly reflecting lead oxide films (Surface Profile Measuring System Dektak from Veeco Instruments). Steps for the profilometric determinations were prepared by etching. First, photoresist was used to protect the selected thin film areas. Diluted hydrochloric acid was then applied to remove the remaining thin film. The optical fitting method developed by Ylilammi and Ranta-aho[90] was used to determine the thicknesses of other film materials. In this method, optical UV-Vis spectroscopy (Hitachi U-2000 double beam spectrophotometer) was used to measure the spectra in the wavelength region of 190-1100 nm. After measurement of the reflectance spectra of the deposited films on Si(100), the thickness was measured by fitting a theoretical spectrum to the measured spectrum.

Crystallinity and crystallite orientation in the films were determined by powder X-ray diffraction (Philips MPD 1880) with Cu-Kα radiation. In the case of $PbZrO_3$ thin films, possible epitaxial growth was investigated by rocking curve measurements (Bruker D8 Advance diffractometer).

Metal ratios were measured with an X-ray fluorescence (XRF) spectrometer (Philips PW 1480) equipped with a Rh X-ray tube. Data analysis was performed with the Uniquant 4.34 program, which utilizes the de Jongh Kappa model.[91] A Rutherford back- scattering (RBS) spectrometer was used to verify the metal ratios obtained by XRF. The RBS measurements were done by Samuli Väyrynen and Eero Rauhala at the University of Helsinki. Atom depth distributions were also studied for lead zirconate, bismuth silicate, and bismuth titanate by RBS. Stoichiometry and possible impurities in some cases were investigated by time-of-flight elastic recoil detection analysis (TOF-ERDA).[92] TOF-ERDA measurements were done by Dr. Timo Sajavaara.

Surface morphology studies were mainly performed with a Nanoscope III atomic force microscope (AFM) from Digital Instruments. The AFM was operated in tapping mode. Roughness values were calculated as root mean square values (rms).

5 Results and discussion

This chapter summarizes the main results of the preparation and characterization of the lead and bismuth oxide thin films. Details of the processes can be found in the original publications.[I-V]

5.1 Lead oxide processes

The existence of a wide ALD window was not confirmed for the Ph_4Pb/O_3 and $Pb(thd)_2/O_3$ processes.[I] Self-limiting growth was nevertheless demonstrated for both processes. In the case of the Ph_4Pb/O_3 process, self-limiting growth was obtained at 250 and 300 °C. The growth rate at 250 °C was 0.13 Å/cycle, but it decreased slightly to 0.10 Å/cycle when depositions were carried out at 300 °C. It is suggested that this decrease was due to the available reaction sites for organometallic precursor, viz. –OH groups in the surfaces.[I] This has also been observed in the case of Cp_3Sc/O_3 process.[93] Possible changes in the number of –OH groups in the ozone-based ALD processes have rarely been studied. In water-based processes increasing the number of –OH groups in the substrate surface is achieved by increasing water dosage.[94] Using water and hydrogen peroxide as additional oxidizer to increase number of –OH groups was tested by Putkonen *et al.*[93] They found out that H_2O_2 as additional oxidizer increased growth rate of Cp_3Sc/O_3 process by 12 % but H_2O as additional oxidizer had no effect. It seems that additional reaction mechanism studies are needed to fully understand this phenomenon.

A significantly higher growth rate of 1.1 Å/cycle was obtained for the self-limiting $Pb(thd)_2/O_3$ process at 150 °C. $Pb(dedtc)_2/O_3$ experiments resulted in lead sulfate thin films, and attempts to thermally decompose the sulfate to oxide by annealing failed.

Lead oxide films crystallized in the PbO_2 stoichiometry rather than the expected PbO. This was believed to happen because ozone is an aggressive oxidant. However, recently Zhao *et al.*[95] obtained films composed of PbO_2 and Pb_3O_4 in a CVD study of the $Pb(thd)_2/O_2$ precursor system at 525 °C when Ir was used as substrate material. At somewhat lower deposition temperature of 420 °C Hendricks *et al.*[96] obtained lead

monoxide by CVD with same precursor system, $Pb(thd)_2/O_2$. Only difference was substrate surface since Hendricks *et al.* used both polycrystalline alumina and sapphire. In our study according to XRD, both successful lead oxide processes resulted in polycrystalline thin films on Si(100). Reflections due to tetragonal and orthorhombic PbO_2 phase were present, and in both cases tetragonal (110) was the most intense reflection. According to the AFM measurements, rms values for the Ph_4Pb/O_3 process varied between 3.9 and 5.3 nm, depending on the deposition temperature and thickness of the films (see Figure 7).

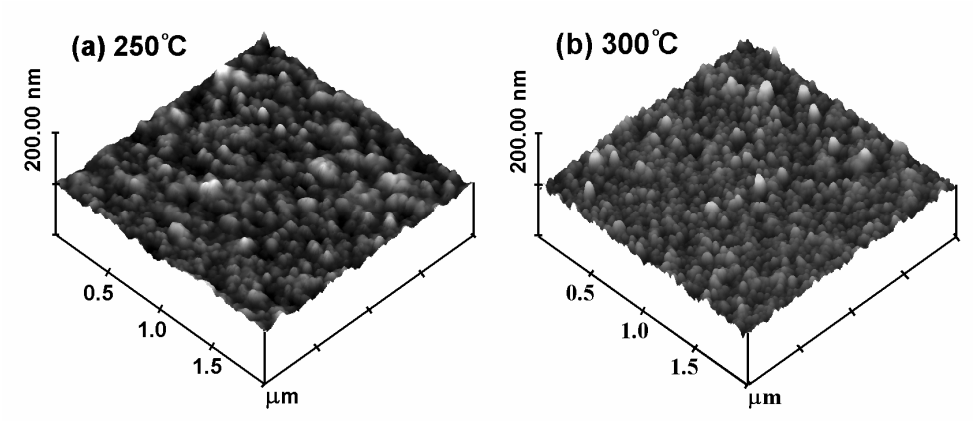

Figure 7. AFM images of PbO_2 films deposited by the Ph_4Pb/O_3 process a) at 250 °C and b) at 300 °C. Thin film thicknesses and rms values were a) 130 nm and 3.9 nm, and b) 90 nm and 4.6 nm, respectively. Image size is 2x2 μm^2.

According to TOF-ERD analyses, the lead to oxygen atomic ratio was near 0.7 in the two successful processes, resulting in an uncertainty of ±3 at.% in the Pb:O ratio. Carbon impurities were 0.5 at.% for the Ph_4Pb/O_3 process but somewhat higher for the $Pb(thd)_2/O_3$ process (1.1 at.%). Hydrogen impurities were below 0.2 at.% in both cases.

5.2 Lead titanate and lead zirconate processes

Ph_4Pb rather than $Pb(thd)_2$ was chosen as lead precursor in the ternary phase experiments, because in the binary lead oxide studies $Pb(thd)_2$ decomposed above deposition temperatures of 200 °C.[I] There were indications that 200 °C was too high a temperature for $Pb(thd)_2$ too, since some of the deposits were black at the edges of the substrate. Probably this was due to carbon contamination from decomposition of the thd-ligand. Deposition temperature below 200 °C is too low considering that other

binary oxide processes have produced the more complex PZT or PLZT, with optimum deposition temperature typically at or above 200 °C.

Lead titanate was produced with the pulsing sequence N x [A x Ph_4Pb/O_3 + B x Ti(O-*i*-Pr)$_4$/H_2O], where N is the number of ternary deposition cycles, A is the number of binary lead oxide cycles and B is number of binary titanium dioxide cycles. A/B is the ratio of the binary processes. For stoichiometric films, A values were 10 and 28 (B=1) at the deposition temperatures of 250 and 300 °C, respectively. Growth rate of the stoichiometric lead titanate at 250 °C was 0.24 Å/cycle. This value is about 115% relative to the rate calculated from the binary oxide processes. In fact, the growth rate was always higher than the calculated value when low proportion of titanium was pulsed. The rate was decreased below the calculated value when the Pb to Ti pulsing ratio was 9:1 or lower. High growth rates as compared with the calculated values were also measured in three recent ALD studies of lead titanate by Watanabe *et al.*[71,74] and Hwang *et al.*[72] Reactivities in oxide processes are surface sensitive and hence the high growth rates are explained by the different surface chemistries in the ternary and binary processes. Also, available adsorption sites or bonding modes may vary, as has been proposed for other ternary oxide ALD processes.[97,98]

The pulsing sequence in the lead zirconate process was N x [A x Ph_4Pb/O_3 + B x Zr(thd)$_4$/O_3].[III] A closely stoichiometric lead zirconate was obtained when A had a value of 7 and B a value of 2 at 275 °C. At the higher deposition temperature of 300 °C, the values for A and B were 6 and 1, respectively. Growth rate of the close to stoichiometric lead zirconate was 0.12 Å/cycle at 275 °C. As in the lead titanate process, also in this process the growth rate was found to depend on the pulsing ratio. A maximum rate 50 % higher than the combined rate for the binary process was obtained when the ratio of Pb to Zr in the films was between 0.9 and 1.25. At ratios below 0.9 and above 1.25, the rate settled to the same value as calculated from separate binary oxides.

Both lead titanate and lead zirconate processes showed a linear dependency of film thickness on the number of cycles, as seen in Figure 8.[II,III] In the case of lead titanate, however, it seems that the data points do not converge at zero. A possible explanation for this behavior could be the incubation period during the initial ALD cycles where the

surface chemistry has a different effect on the growth rate, as seen in the study by Hwang *et al.*[72] However, it should be noted that Hwang *et al.* used Ir electrode as a substrate and this different type of surface compared to Si substrates certainly has an influence on the growth, too.

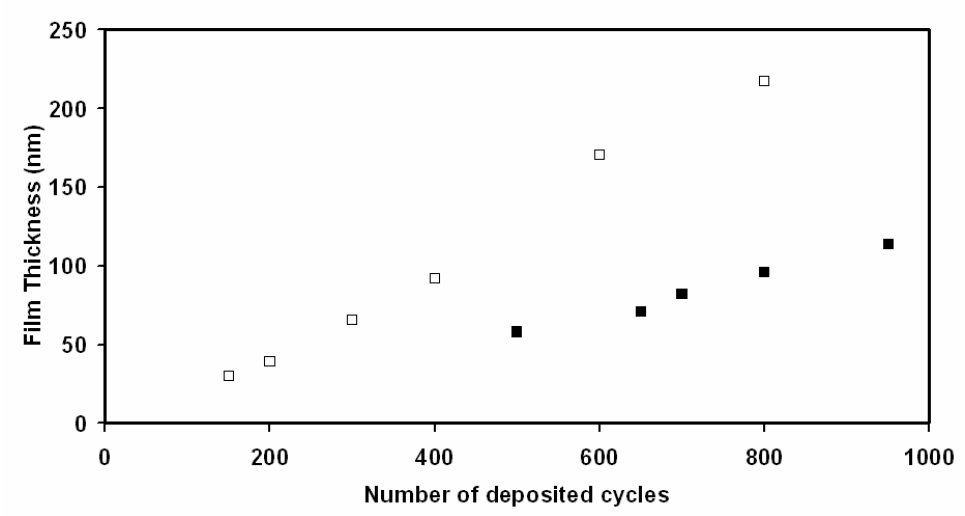

Figure 8. Dependence of film thickness on the number of deposited cycles. The open symbols refer to lead titanate deposited at 250 °C and the solid symbols to lead zirconate deposited at 275 °C.

Both ternary lead oxide processes yielded smooth and uniform thin films, which, however, according to surface morphologies analyzed by AFM appeared to have rougher surfaces than those obtained in the binary processes.[II,III] In previous studies, rms values of 4-5.5 nm were obtained for 100-130-nm-thick binary oxide thin films.[I,73,86] Values of about 24 nm were obtained for the as-deposited stoichiometric lead titanate films, and after annealing the values were even higher.[II] In the case of lead zirconate, roughness was highly dependent on the metal ratio of the films.[III] The rms value of zirconium-deficient films (Pb:Zr ratio 1.1) was as high as 23 nm for as-deposited film. However, it was just 7 nm in the as-deposited lead-deficient films (Pb:Zr ratio 0.9). As with the lead titanate films, annealing reduced the rms values of the lead zirconate films. In previous studies on the mobility and diffusion of lead, it was concluded that the mobility of lead is high.[99,100] Thus, high mobility of lead in the thin films could be the reason for agglomeration and one explanation of the high roughness values, especially in the films with high lead concentrations.

Lead titanate films contained less than 0.2 at.% carbon and less than 0.1-0.5 at.% hydrogen impurities as detected by TOF-ERDA.[II] A small tin impurity was detected in lead zirconate films by RBS.[III] Probable the tin originates from the impurities in the lead precursor (97% purity). Element distribution in depth was studied for lead zirconate by RBS. The zirconium concentration was more or less constant throughout the film, but the Pb concentration increased slightly with depth in the as-deposited films. The composition of the films remained relatively stable during the annealing at 600 °C.

The effect of annealing. According to XRD as-deposited stoichiometric lead titanate films were amorphous, while the lead zirconate films crystallized into various crystalline lead and zirconium phases.[II,III] Annealing was necessary to obtain crystalline perovskite phases.

Annealing of lead titanate films was studied in nitrogen and oxygen atmospheres with annealing temperatures between 600 and 900 °C.[II] The annealing time was kept constant at 10 min. Since oxygen was found to promote the crystallization of the $PbTiO_3$ phase, the crystallization and preferred orientations of $PbTiO_3$ were studied more carefully in this atmosphere (Figure 9). Crystallization of perovskite phase in the nearly stoichiometric films was initiated above 550 °C when films were deposited at 250 °C. Slightly lead-rich films (Ti:Pb atomic ratios of 0.6-0.8) contained only polycrystalline $PbTiO_3$ with preferred orientation (101). Otherwise additional low intensity peaks together with peaks of $PbTiO_3$ were detected. Probably these other peaks belonged to lead oxide and $PbTi_3O_7$ phases. Films deposited at 300 °C required higher annealing temperatures than the films deposited at lower temperatures.

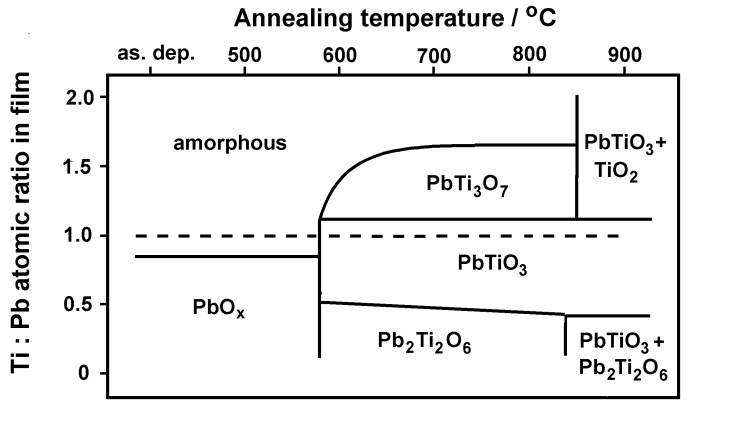

Figure 9. Summary of the influence of composition and annealing temperature on crystalline phases detected in Pb-Ti-O films by XRD. Depositions were done at 250 °C and annealing in an O_2 atmosphere.[II]

The perovskite $PbZrO_3$ phase was not observed in the films deposited on Si(100) or MgO-buffered Si(100) even after annealing.[III] The same negative result was obtained in a CVD study.[101] High crystallization was confirmed after deposition on single crystal $SrTiO_3$ substrates and annealing at 600 °C in O_2 atmosphere.[III] The most intense reflection was (400). Rocking curve measurements were performed to obtain information about possible epitaxial growth. Rocking curve maxima were, in fact, obtained but the peaks were broad and hence indicated strong texture rather than epitaxiality.

A slight excess of lead, which enhanced the crystallinity, was observed in both ternary lead oxide studies.[II,III] The same has been observed in other ALD and CVD studies, where an excess of Pb has been reported to have a favorable affect on the crystallization of ternary lead oxides.[72,102]

5.3 Bismuth silicate and bismuth titanate processes

Bismuth silicate process. A new bimetallic precursor $Bi(CH_2SiMe_3)_3$ was introduced for the deposition of bismuth silicate films.[IV] With O_3 as oxygen source, a constant growth rate of 0.40 Å/cycle was obtained between deposition temperatures of 250 and 350 °C. In addition, water and molecular oxygen were tested as oxygen sources, but no film growth was observed. With ozone, a self-limiting growth, as well as the existence

of a linear relationship between the film thickness and the number of deposition cycles, were confirmed at deposition temperature of 250 °C.

The silicon to bismuth atomic ratio was observed to increase with deposition temperature.[VI] Within the ALD window of 250-350 °C, a ratio of about 2 was observed by XRF and RBS. A second bismuth precursor, $BiPh_3$, was added to the ALD process in an attempt to increase the bismuth content in the bismuth silicate films.[V] Through change in the pulsing ratios of these two $BiPh_3/O_3$ and $Bi(CH_2SiMe_3)_3/O_3$ processes, it was possible to achieve almost linear control of the bismuth content in the bismuth silicate process.

Even though the $Bi(CH_2SiMe_3)_3/O_3$ process resulted in silicon-rich films, crystallization of this process was studied in detail.[IV] The as-deposited films were amorphous and annealing was performed in the range of 400-1000 °C. For films deposited at 250 °C, crystallization started at 600 °C in N_2 and O_2 atmospheres. Films crystallized in the orthorhombic Bi_2SiO_5 form with preferred a-axis orientation. Minor peaks of the $Bi_{12}SiO_{20}$ phase were observed as well, but intensities were below 1% as compared with those of the Bi_2SiO_5 phase. After annealing at 1000 °C, polycrystalline cubic $Bi_4Si_3O_{12}$ was observed. Annealing temperature has previously been observed to affect the preferred crystalline orientations. Kim *et al.*[103] obtained the oriented Bi_2SiO_5 phase at annealing temperatures of 800 °C and below, whereas only the reflections of polycrystalline $Bi_4Si_3O_{12}$ were present above 800 °C. This is a slightly lower temperature than the 1000 °C used in our study to crystallize the $Bi_4Si_3O_{12}$ phase. The annealing temperature of 1000 °C was also found to be too high to maintain good film quality.

The silicon to bismuth atomic ratio in the crystalline phases, viz. Bi_2SiO_5, $Bi_{12}SiO_{20}$, and $Bi_4Si_3O_{12}$, was lower than the values obtained by XRF and RBS.[IV,V] Discrepancies in the Si/Bi ratios may be explained in terms of the presence of amorphous material. Thus, after annealing, the films may consist of a crystalline bismuth silicate phase together with an amorphous silicon oxide or other silicon-rich phase.

Crystallization of Bi-Si-O films was studied on different substrate surfaces.[V] Films were deposited on sapphire and on MgO-, ZrO_2- and YSZ-buffered Si(100) and then

annealed to enhance crystallinity. The best crystallinity was obtained when films were annealed at 800 °C. Films were *a*-axis oriented orthorhombic Bi_2SiO_5, and no additional reflections were observed. As can be seen in Figure 10, the most intense reflection, viz. (200) was 10 times as strong on MgO-buffered Si(100) as on Si(100) without the buffer layer. It was also considerably stronger on sapphire and the other buffered substrates than on pure Si(100) (1.3-2.6 times stronger).

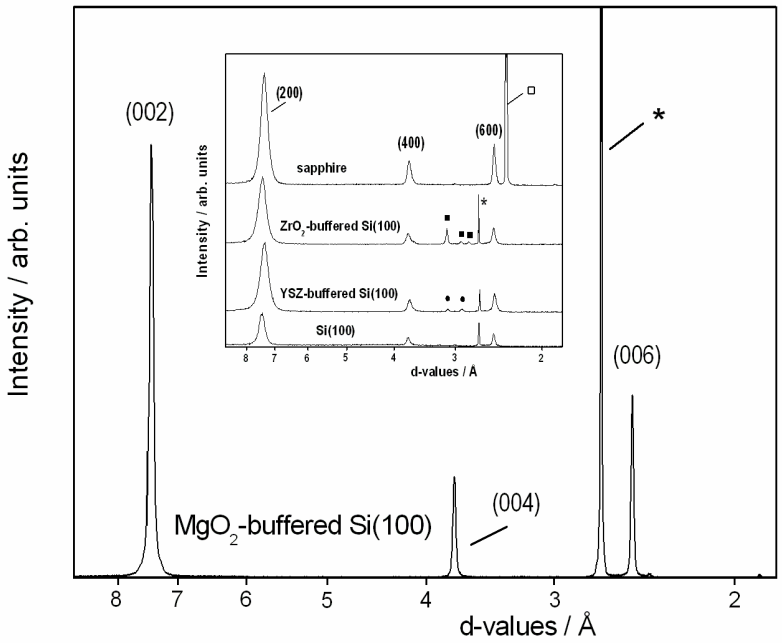

Figure 10. XRD pattern of Bi_2SiO_5 thin film deposited on MgO-buffered Si(100) and annealed at 800 °C. For comparison the inset shows patterns for films deposited on sapphire, ZrO_2-buffered Si(100), YSZ-buffered Si(100), and Si(100). Asterisk (*) denotes reflections from the Si-substrate, open square (□) reflections from sapphire substrate, solid square (■) reflections from ZrO_2 buffer layer, and solid circles (●) reflections from the YSZ buffer layer.

Impurity contents in bismuth silicate films were low according to TOF-ERDA.[IV] Carbon and hydrogen contents were less than 0.2 at.% and 0.1 at.%, respectively. Distribution of bismuth in as-deposited as well as in annealed samples was studied by RBS.[IV] The as-deposited film shows an almost even distribution of bismuth and silicon. After annealing at 800 °C the distribution changed dramatically. The silicon to bismuth ratio was high on the surface, decreased towards the middle of the film, and increased again towards the interfacial region of the film and the substrate. Bismuth diffusion into

the SiO_2 and silicon substrate has been demonstrated to take place above 600 °C.[104-106] It is suggested therefore, that also in this study the differences in elemental distributions after the annealing are due to the diffusion of bismuth towards the silicon substrate rather than evaporation.[III]

Bismuth titanate process. Usually binary oxide ALD processes are established before the deposition of ternary oxides. However, attempts to deposit bismuth oxide by ALD using $BiPh_3$ as Bi precursor failed.[V,77] In further studies, it was demonstrated that, even though this precursor did not work for binary processes it was still possible to grow the ternary bismuth titanate phase.[V,77] Possible reason for that is the catalytic nature of titanium dioxide that enhances the reactivity of the $BiPh_3$ precursor.[77] In our study, the $BiPh_3/O_3$ process was used together with the $Ti(O\text{-}i\text{-}Pr)_4/H_2O$ process to produce ternary bismuth titanate thin films at deposition temperature of 250 °C. Films were deposited using the pulsing sequence N x [A x $BiPh_3/O_3$ + $Ti(O\text{-}i\text{-}Pr)_4/H_2O$]. The bismuth to titanium atomic ratio was changed when the value of A was altered. With A=10, the Ti to Bi atomic ratio was 0.28,[V] which is much lower than the minimum value of 1.6 obtained by Schuisky *et al.*[77] with H_2O as the oxygen source for the Bi precursor. The different oxygen source, ozone[V] vs. water[77], probably explains the lower value.

Crystallinity was studied after annealing in three different atmospheres: N_2, O_2, and air. Annealing in air was done in a tube furnace with much slower annealing rate than in the rapid thermal annealing (RTA) oven. Also, the annealing time in the tube furnace was 30 min, compared with only 10 min in the RTA oven. Probably because of the slow annealing rate and longer annealing time, 00k oriented $Bi_4Ti_3O_{12}$ phase was formed at 900 °C when annealing was done in air. A temperature of 1000 °C was required when annealing was done in N_2 and O_2 in the RTA oven. 00k oriented $Bi_4Ti_3O_{12}$ was also observed at 900 °C, but intensities were much lower than in air. Figure 11 shows the XRD pattern of a thin film annealed in N_2 atmosphere at 1000 °C, where the most textured film was achieved.

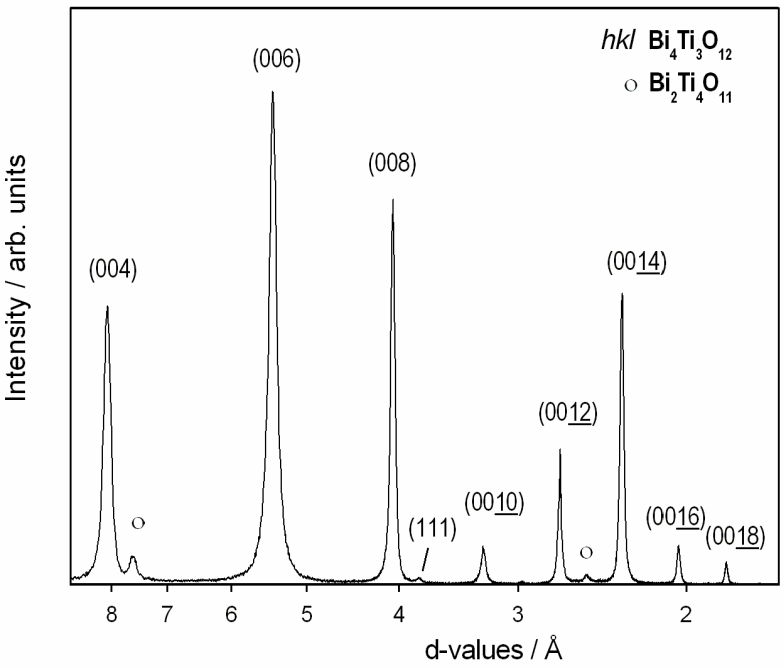

Figure 11. XRD patterns for a 95-nm bismuth titanate film on Si(100) substrate annealed at 1000 °C in N_2 atmosphere.

Oriented crystalline $Bi_4Ti_3O_{12}$ was observed with an excess of bismuth in the films. Nearly stoichiometric films crystallized in $Bi_4Ti_3O_{12}$ phase, but also other minor peaks, belonging to $Bi_2Ti_2O_7$, $Bi_2Ti_4O_{11}$, and $Bi_2O_{2.33}$, were detected. If the bismuth content in the films decreased (Ti/Bi atomic ratios above 1.0), the $Bi_2Ti_2O_7$ phase was crystallized.

As in the Bi-Si-O thin films, RBS analyses of the Bi-Ti-O thin films revealed an almost even distribution of metals in the as-deposited films.[V] After annealing at 800 °C the nearly stoichiometric sample showed only slight changes in the depth distributions. However, strong redistribution of bismuth and titanium was observed in bismuth-rich films as well as in films annealed at 1000 °C. Redistribution was away from the interface and towards the surface.

Visual inspection suggested that annealing in nitrogen atmosphere is preferable for bismuth titanate films, as deterioration of the films occurs in oxidizing atmosphere. The crystallinity was continuously improved in N_2 up to the annealing temperature of 1000

°C. Films were visually shiny, and adhesion of the films was good even after annealing at 1000 °C. Considering that annealing temperature of 1000 °C is too high for most applications and that the RBS data showed a severely uneven elemental distribution at this temperature, a lower annealing temperature or a buffer layer must be recommended. It should also be noted that random nucleation improves the electrical properties of the films.[21]

The surface roughness of as-deposited films increased along with the bismuth content (see Figure 12). A probable reason for these higher rms values is the surface diffusion of bismuth.[21] With titanium to bismuth ratios of 0.28 and 1.28, the rms values were 4.6 and 1.8 nm, respectively. Interestingly, after annealing at 800 °C in N_2 atmosphere, the rms values were nearly the same - 6 nm - independent of the atomic ratio.

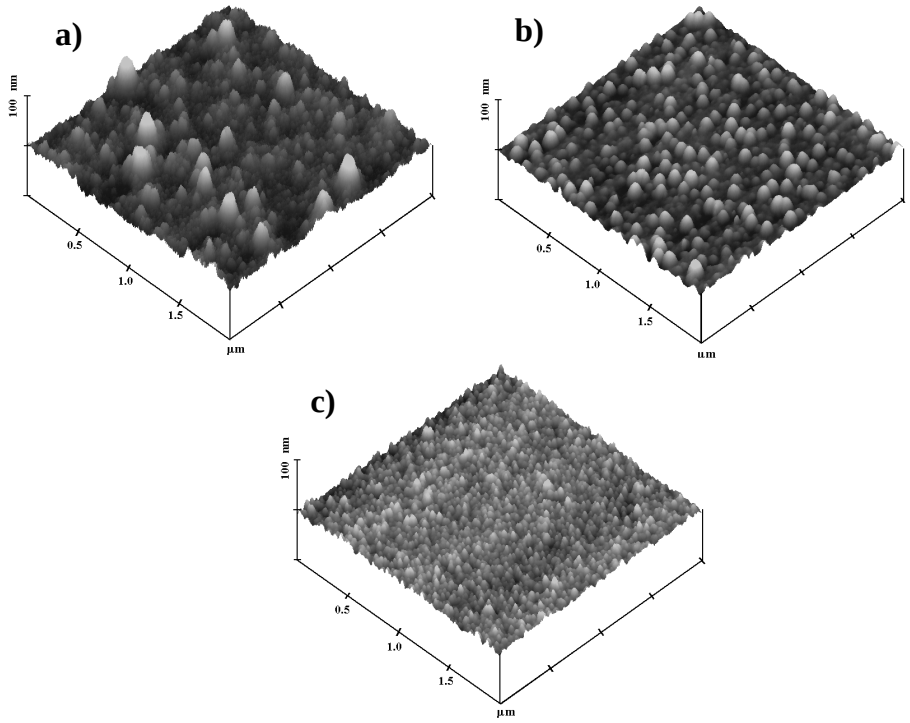

Figure 12. AFM images of the as-deposited Bi-Ti-O thin films. The Ti/Bi atomic ratio and rms values are a) 0.28 and 4.6 nm, b) 0.71 and 2.5 nm, and c) 1.28 and 1.8 nm, respectively. Image size is 2x2 μm^2. Thicknesses of the films were 95 (a) and 100 nm (b,c).[V]

According to the RBS data, mobility of metals was higher in samples where bismuth content was higher. Measured by AFM, higher bismuth content also resulted in a

rougher surface. It can tentatively be concluded that an excess of bismuth enhances the mobility of metals both within the films and on their surface so increasing the surface roughness, but additional studies are needed to fully understand this phenomenon.

6 Conclusions

Oxides containing two or more cations and whose stoichiometry has to be accurately controlled are among the most challenging materials for ALD. The lack of a good binary ALD process for even one of the cations in a multication oxide means that much work must be done to achieve workable overall multication process. In the present work, new ternary oxide processes were described for lead and bismuth. The following conclusions are drawn in regard to the different processes.

Ph_4Pb and $Pb(thd)_2$, together with ozone, were demonstrated to be useful precursors for lead processes. Thus, both of these binary processes can be further exploited in ternary processes. The growth rate of Ph_4Pb was fairly low and it decreased with increasing deposition temperature, but the process was self-limiting. In the case of $Pb(thd)_2$, the growth was self-limiting at the rather low temperature of 150 °C and decomposition started at 200 °C. Both processes produced polycrystalline PbO_2 thin films.

It was demonstrated that stoichiometric ternary lead oxides can be obtained with a careful optimization of the binary oxide pulsing ratios. Probably because of the low growth rate of the Ph_4Pb/O_3 process, a high pulsing ratio was required to obtain stoichiometric $PbTiO_3$ and $PbZrO_3$ thin films. In both ternary processes the surface chemistry was different from that in the binary processes, and this probably explains why the growth rate in the ternary processes was higher than the theoretical values calculated from the binary processes. The perovskite phase was obtained after annealing on silicon substrate in the case of $PbTiO_3$ and on $SrTiO_3$ substrate in the case of $PbZrO_3$. In both cases an excess of lead improved the crystallinity, but unfortunately, in the case of $PbZrO_3$ the roughness was increased along with increase in the lead content.

A new bimetallic precursor was introduced for the bismuth silicate ALD growth. With use of an additional bismuth precursor, it was possible to control the metal ratio of the Bi-Si-O thin films. The Bi_2SiO_5 phase was crystallized, after annealing, on Si(100). Crystallization was improved on some other surfaces, with the best results obtained on MgO-buffered Si(100).

Even though the development of a binary bismuth process was not successful, the ternary bismuth titanate $Bi_4Ti_3O_{12}$ could be grown by ALD. Bismuth titanate thin films with different metal ratios could be processed by changing the ratio of the bismuth oxide cycles to the titanium oxide cycles. Different crystalline compounds were crystallized depending on the metal ratio in the films. As-deposited films were amorphous and the annealing was necessary to crystalline these phases. A higher content of bismuth than titanium in the bismuth titanate films resulted in rougher surfaces.

The depth distribution of bismuth was studied for both ternary bismuth oxide processes. Both as-deposited ternary thin films showed an even distribution of metals. While annealing changed the distribution of the metals, the degree of change was independent of the annealing temperature as well as of the metal ratio of the films.

For the future, it would be worthwhile to expand the range of available precursors for both lead and bismuth and thus improve and widen the possibilities to grow ternary and more complex oxides by ALD. The present results are promising, however, and give valuable information on complex oxide growth and properties of the films for further studies and eventual applications.

7 References

1. Bhalla, A.S., Guo R. ,and Roy, R., The perovskite structure – a review of its role in ceramic science and technology, *Mat. Res. Innovat.* **4** (2000) 3.

2. Haertling, G.H., Ferroelectric ceramics: history and technology, *J. Am. Ceram. Soc.* **82** (1999) 797.

3. Auciello, O., Scott, J.F., and Ramesh, R., The physics of ferroelectric memories, *Physics Today* **7** (1998) 22.

4. Bharadwaja, S.S.N., and Krupanidhi, S.B., Growth and study of antiferroelectric lead zirconate thin films by pulsed laser ablation, *J. Appl. Phys.* **86** (1999) 5862.

5.Ritala, M., and Leskelä, M., Atomic layer deposition. In *Handbook of Thin Film Materials*, Vol. 1, Ed. H.S. Nalwa, Academic Press, San Diego, USA, 2002, p. 103.

6.Galasso, F.S., *Perovskite and high T_c superconductors*, Gordon and Breach Science Publisher, New York 1990, p.293.

7. Kim, K., and Song, Y.J., Integration technology for ferroelectric memory devices, *Microelectron. Reliab.* **43** (2003) 385.

8. Lindner, J., Schumacher, M., Dauelsberg, M., Schienle, F., Miedl, S., Burgess, D., Merz, E., Strauch, G., and Juergensen, H., Deposition of electroceramic thin films by MOCVD, *Adv. Mater. Opt. Electron.* **10** (2000) 163.

9. Woodward, P.M., Octahedral tilting in perovskites. I. Geometrical considerations, *Acta Crystallogr., Sect. B: Struct. Sci.* **53** (1997) 32.

10. Hervoches, C.H., and Lightfoot, P., A variable-temperature powder neutron diffraction study of ferroelectric $Bi_4Ti_3O_{12}$, *Chem. Mater.* **11** (1999) 3359.

11. Aurivillius, B., Mixed bismuth oxides with layer lattices. I. Structure type of $CaNb_2Bi_2O_9$, *Ark. Kemi* **1** (1949) 463.

12. Aurivillius, B., Mixed bismuth oxides with layer lattices. II. Structure of $Bi_4Ti_3O_{12}$, *Ark. Kemi* **1** (1949) 499.

13. Izumi, F., and Dilanian, R.A., *Recent Research Developments in Physics*, Vol. 3, Part II, Transworld Research Network, Trivandrum 2002, pp. 699-726.

14. Kaul, A., Gorbenko, O., Novojilov, M., Kamenev, A., Bosak, A., Mikhaylov, A., Boytsova, O., and Kartavtseva, M., Epitaxial stabilization – a tool for synthesis of new thin film oxide materials, *J. Cryst. Growth* **275** (2005) e2445.

15. Scott, J.F., and Paz De Araujo, C.A., Ferrolelectric memories, *Science* **246** (1989) 1400.

16. *International Technology Roadmap for Semiconductors*, Front End Processes, 2005 Edition http://www.itrs.net/, 14.7.2006.

17. Dawber, M., Rabe, K.M., and Scott, J.F., Physics of ferroelectric oxides, *Rev. Mod. Phys.* **77** (2005) 1083.

18. Lee, S., and Kim, K., Current development status and future challenges of ferroelectric random access memory technologies, *Jpn. J. Appl. Phys.* **45** (2006) 3189.

19. Lee, J.K., Park, Y., and Chung, I., Investigation of hydrogen induced degradation in $Pb(Zr_xTi_{1-x})O_3$ thin film capacitors for the application of memory devices, *J. Appl. Phys.* **92** (2002) 2724.
20. Kohlstedt, H., Mustafa, Y., Gerber, A., Petraru, A., Fitsilis, M., Meyer, R., Böttger, U., and Waser, R., Current status and challenges of ferroelectric memory devices, *Microelectron. Eng.* **80** (2005) 296.
21. Vehkamäki, M., Hatanpää T., Kemell, M., Ritala, M., and Leskelä, M., Atomic layer deposition of ferroelectric bismuth titanate $Bi_4Ti_3O_{12}$ thin films, *Chem. Mater.* **18** (2006) 3883.
22. Muralt, P., Ferroelectric thin films for micro-sensors and actuators: a review, *J. Micromech. Microeng.* **10** (2000) 136.
23. Re, T.-L., Zhao, H.-J., Liu, L.-T., and Li, Z.-J., Piezoelectric and ferroelectric films for microelectronic applications, *Mater. Sci. Eng.* **B99** (2003) 159.
24. Cheng, Z., Kannan, C.V., Ozawa, K., Kimura, H., and Wang, X., Orientation dependent ferroelectric properties in samarium-doped bismuth titanate thin films grown by the pulsed-laser-ablation method, *Appl. Phys. Lett.* **89** (2006) 032901.
25. Adachi, Y, Su, D., Muralt, P., and Setter, N., Ferroelectric and piezoelectric properties of lanthanoid-substituted $Bi_4Ti_3O_{12}$ thin films grown on (111)Pt and (100)IrO_2 electrodes, *Appl. Phys. Lett.* **86** (2005) 172904.
26. Suyal, G., Bharadwaja, S.S.N., Cantoni, M., Damjanovic, D., and Setter, N., Properties of chemical solution deposited polycrystalline neodymium-modified $Bi_4Ti_3O_{12}$, *J. Electroceram.* **9** (2002) 187.
27. Shi, C., Meidong, L., Churong, L., Yike, Z., and Da Costa, J., Investigation of crystallographic and pyroelectric properties of lead-based perovskite-type structure ferroelectric thin films, *Thin Solid Films* **375** (2000) 288.
28. Sun, L.L., Tan, O.K., and Zhu, W.G., $Pb(Zr_{0.3}Ti_{0.7})O_3/PbTiO_3$ multilayer thin films for pyroelectric infrared sensor applications, *J. Appl. Phys.* **99** (2006) 094108.
29. Schreiter, M., Gabl, R., Lerchner, J., Hohlfeld, C., Delan, A., Wolf, G., Bluher, A., Katzschner, B., Mertig, M., and Pompe, W., Functionalized pyroelectric sensors for gas detection, *Sens. Actuators, B* **119** (2006) 255.
30. Akai, D., Hirabayashi, K., Yokawa, M., Sawada, K., Taniguchi, Y., Murashige, S., Nakayama, N., Yamada, T., Murakami, K., and Ishida, M., *Sens. Actuators, A* **130-131** (2006) 111.
31. Buchanan, R.C., Palan, R., Ghaffari, A., Tran, K., and Sundeen, J.E., Orientation effects on polarization and pyroelectric properties of ferroelectric thin films on Si, *J. Electrochem. Soc.* **21** (2001) 1577.
32. Hu, S.H., Chen, J., Hu, Z.G., Wang, G.S., Meng, X.J., Chu, J.H., and Dai, N., The optical properties of $Bi_{3.25}La_{0.75}Ti_3O_{12}$ thin films with different thickness prepared by chemical solution deposition, *Mater. Res. Bull.* **39** (2004) 1223.
33. Gardin, J., Leduc, D., Schneider, T., Lupi, C., Averty, D., and Gundel, H.W., Optical characterization of PZT thin films for waveguide applications, *J. Eur. Ceram. Soc.* **25** (2005) 2913.
34. Leng, W.J., Yang, C.R., Ji, H., Zhang, J.H., Tang, J.L., and Chen, H.W., Electrical and optical properties of lanthanum-modified lead zirconate titanate thin films by radio-frequency magnetron sputtering, *J. Appl. Phys.* **100** (2006) 106102.

35. Ritala, M., and Leskelä M., Atomic layer deposition of thin films for microelectronics, *Proceedings on the International Symposium of CVD XVI and EUROCVD 14*, Ed. Allendorf, M.D., Maury, F. and Teyssandier F., Paris 2003, p. 479.
36. Suntola T., and Antson, J., Method for producing compound thin films, *US pat.* 4,058,430 15.11.1977.
37. Puurunen, M., Surface chemistry of atomic layer deposition: A case study for the trimethylaluminum/water process, *J. Appl. Phys.* **97** (2005) 121301.
38. Niinistö, L., Päiväsaari, J., Niinistö, J., Putkonen, M., and Nieminen, M., Advanced electronic and optoelectronic materials by Atomic Layer Deposition: an overview with special emphasis on recent progress in processing of high-*k* dielectrics and other oxide materials, *Phys. Stat. Sol. A* **201** (2004) 1443.
39. Leskelä, M., and Ritala, M., Atomic layer deposition chemistry: recent developments and future challenges, *Angew. Chem. Int. Ed.* **42** (2003) 5548.
40. Niinistö, L., Ritala, M., and Leskelä M., Synthesis of oxide thin films and overlayers by atomic layer epitaxy for advanced applications, *Mater.Sci. Eng.* **B41** (1996) 23.
41. Suntola, T., Atomic layer epitaxy, *Mater. Sci. Reports* **4** (1989) 261.
42. Putkonen, M., and Niinistö, L., Organometallic precursors for atomic layer deposition, *Top. Organomet. Chem.* **9** (2005) 125.
43. Ritala, M., Kukli, K., Rahtu, A., Räisänen, P.I., Leskelä, M., Sajavaara, T., and Keinonen, J., Atomic layer deposition of oxide thin films with metal alkoxides as oxygen source, *Science* **288** (2000) 319.
44. Lee, W.-J., You, I.-K., Ryu, S.-O., Yu B.-G., Cho, K.-I., Yoon, S.-G., and Lee, C.-S., $SrTa_2O_6$ thin films deposited by plasma-enhanced atomic layer deposition, *Jpn. J. Appl. Phys.* **40** (2001) 6941.
45. Chae, B.-G., Lee, W.-J., You, I.-K., Ryu, S.-O., Jung, M.-Y., and Yu B.-G., New high-*k* $SrTa_2O_6$ gate dielectrics prepared by plasma-enhanced atomic layer chemical vapor deposition, *Jpn. J. Appl. Phys.* **41** (2002) L729.
46. Vehkamäki, M., Ritala, M., Leskelä, M., Jones, A.C., Davies H.O., Sajavaara, T., and Rauhala E., Atomic layer deposition of strontium tantalate thin films from bimetallic precursors and water, *J. Electrochem. Soc.* **151** (2004) F69.
47. Shin, W.-C., Ryu, S.-O., You, I.-K., Yu, B.-G., Lee, W.-J., Choi, K.-J., and Yoon, S.-G., Plasma-enhanced atomic layer deposition of $SrTa_2O_6$ thin films using $Sr[Ta(OC_2H_5)_5(OC_2H_4OCH_3)]_2$ as precursor, *J. Eletrochem. Soc.* **151** (2004) C292.
48. Vehkamäki, M., Hatanpää T., Ritala, M., and Leskelä, M., Bismuth precursors for atomic layer deposition of bismuth-containing oxide films, *J. Mater. Chem.* **14** (2004) 3191.
49. Shin, W.C., Ryu,S.O., You, I.K., Yoon, S.M., Cho, S.M., Lee, N.Y., Kim, K.D., Yu, B.G., Lee, W.J., Choi, K.J., and Yoon, S.G., Low voltage switching characteristics of 60 nm thick $SrBi_2Ta_2O_9$ thin films deposited by plasma-enhanced ALD, *Electrochem. Solid-State Lett.* **7** (2004) F31.
50. Kijima, T., New low temperature preparation of ferroelectric $Bi_4Ti_3O_{12}$ thin films by MOCVD method, *Integr. Ferroelectrics* **26** (1999) 93.
51. Nam, W.-H., and Rhee, S.-W., Atomic layer deposition of hafnium silicate thin films using $HfCl_2[N(SiMe_3)_2]_2$ and H_2O, *Electrochem. Solid-State Lett.* **7** (2004) C55.

52. Kang, S.-W., Rhee, S.-W., and George S.M., Infrared study of atomic layer deposition mechanism for hafnium silicate thin films using $HfCl_2[N(SiMe_3)_2]_2$ and H_2O, *J. Vac. Sci. Technol.* **A22** (2004) 2392.
53. Scarel, G., Wiemer, C., Tallarida, G., Spiga, S., Seguini, G., Bonera, E., Fanciulli, M., Lebedinskii, Y., Zenkevich, A., Pavia, G., Fedushkin, I.L., Fukin, G.K., and Domrachev, G.A., Atomic layer deposition of Lu silicate films using $[(Me_3Si)_2N]_3Lu$, *J. Electrochem. Soc.* **153** (2006) F271.
54. Nam, W.-H., and Rhee, S.-W., Atomic layer deposition of ZrO_2 thin films using dichlorobis[bis-(trimethylsilyl)amido]zirconium and water, *Chem. Vap. Deposition* **10** (2004) 201.
55. Schultz, M., The end of the road for silicon?, *Nature* **399** (1999) 729.
56. Kim, W.-K., Nam, W.-H., Kim, S.-H., and Rhee, S.-W., Atomic layer chemical vapor deposition (ALCVD) of Hf and Zr silicate and aluminate high-*k* gate dielectric for next generation nano devices, *J. Chem. Eng. Jpn.* **38** (2005) 578.
57. Kim, W.-K., Kang, S.-W., Rhee, S.-W., Lee, N.-I., Lee, J.-H., and Kang, H.-K., Atomic layer deposition of zirconium silicate films using zirconium tetrachloride and tetra-*n*-butyl orthosilicate, *J. Vac. Sci. Technol.* **A20** (2002) 2096.
58. Kim, W.-K., Kang, S.-W., and Rhee, S.-W., Atomic layer deposition of zirconium silicate films using zirconium tetra-*tert*-butoxide and silicon tetrachloride, *J. Vac. Sci. Technol.* **A21** (2003) L16.
59. Conley Jr., J.F., Ono, Y., and Tweet, D.J., Pulsed deposition of metal-oxide thin films using dual metal precursors, *Appl. Phys. Lett.* **84** (2004) 398.
60. Gordon, R.G., Becker, J., Hausmann, D., and Suh, S., Vapor deposition of metal oxides and silicates: Possible gate insulator for future microelectronics, *Chem. Mater.* **13** (2001) 2463.
61. Kim, W.-K., Kang, S.-W., Rhee, S.-W., Lee, N.-I., Lee, J.-H., and Kang, H.-K., Atomic layer deposition of hafnium silicate films using hafnium tetrachloride and tetra-*n*-butyl orthosilicate, *J. Vac. Sci. Technol.* **A22** (2004) 1285.
62. Funakubo, H., Watanabe, T., Morioka, H., Nagai, A., Takahiro, O., Suzuki, M., Uchida, H., Kouda, S., and Saito K., Polarization of $Pb(Zr,Ti)O_3$ and $Bi_4Ti_3O_{12}$-based ferroelectrics, *Mater. Sci. Eng. B* **118** (2005) 23.
63. Leskelä, M., Niinistö, L., Niemelä, P., Nykänen, E., Soininen, P., Tiitta, M., and Vähäkangas, J., Preparation of lead sulfide thin films by the atomic layer epitaxy process, *Vacuum* **41** (1990) 1457.
64. Nykänen, E., Laine-Ylijoki, J., Soininen, P., Niinistö, L., Leskelä, M., and Hubert-Pfalzgraf, L.G., Growth of PbS thin films from novel precursors by atomic layer epitaxy, *J. Mater. Chem.* **4** (1994) 1409.
65. Nykänen, E., Lehto, S., Leskelä, M., Niinistö, L., and Soininen, P., Blue electroluminescence in Pb^{2+} doped CaS and SrS thin films, in: V.P. Singh, J.C. McClure (Eds.), Electroluminescence, *Proceedings of the Sixth International Workshop on Electroluminescence*, El Paso, Texas, U.S.A, May 11-13, 1992, pp. 199-204.
66. Yun, S.J., Kim Y.S., and Park, S.-H.K., Fabrication of CaS:Pb blue phosphor by incorporating dimeric Pb^{2+} luminescent centers, *Appl. Phys. Lett.* **78** (2001) 721.
67. Yun, S.J., Park, S.-H.K., and Park, J.-B., Electron beam induced degradation of CaS:Pb thin film phosphor grown by atomic layer deposition, *Electrochem. Solid-State Lett.* **6** (2003) C30.
68. Kim, Y.S., Park S.-H.K., and Yun S.J., Low-voltage dc thin-film electroluminescence with an indium-tin-oxide/CaS:Pb/ZnS/Al structure, *Jpn. J. Appl. Phys.* **42** (2003) L520.

69. Kim, Y.S., and Yun, S.J., Photoluminescence properties of Pb^{2+} centres in CaS:Pb thin films, *J. Phys.: Condens. Matter.* **16** (2004) 569.

70. Ihanus, J., Hänninen, T., Hatanpää, T., Ritala, M., and Leskelä, M., Electroluminescent SrS and BaS thin films deposited by ALD using cyclopentadienyl precursors, *J. Electrochem. Soc.* **151** (2004) H221.

71. Watanabe, T., Hoffmann-Eifert, S., Hwang, C.S., and Waser, R., Liquid-injection atomic layer deposition of TiO_x and Pb-Ti-O films, *J. Electrochem. Soc*. **153** (2006) F199.

72. Hwang, G.W., Lee, H.J., Lee, K., and Hwang, C.S., Atomic layer deposition and electrical properties of $PbTiO_3$ thin films using metal-organic precursors and H_2O, *J. Electrochem Soc.* **154** (2007) G69.

73. Ritala, M., Leskelä, M., Niinistö, L, and Haussalo, P., Titanium isopropoxide as a precursor in atomic layer epitaxy of titanium dioxide thin films, *Chem. Mater.* **5** (1993) 1174.

74. Watanabe, T., Hoffmann-Eifert, S., Shaobo, M., Jia, C., and Waser, R., Growth of ternary $PbTiO_x$ films in a combination of binary oxide atomic layer depositions, *J. Appl. Phys.* **101** (2007) 014114-1.

75. Hwang, G.W., Kim, W.D., Min, Y.-S., Cho, Y.J., and Hwang, C.S., Characteristics of amorphous $Bi_2Ti_2O_7$ thin films grown by atomic layer deposition for memory capacitor applications, *J. Electrochem. Soc.* **153** (2006) F20.

76. Min, Y.-S., Cho, Y.J., Asanov, I.P., Han, J.H., Kim, W.D., and Hwang, C.S., $Bi_{1-x-y}Ti_xSi_yO_z$ (BTSO) thin films for dynamic random access memory capacitor applications, *Chem. Vap. Deposition* **11** (2005) 38.

77. Schuisky, M., Kukli, K., Ritala, M., Hårsta, A., and Leskelä, M., Atomic layer CVD in the Bi-Ti-O system, *Chem. Vap. Deposition* **6** (2000) 139.

78. Schuisky, M., *CVD and ALD in the Bi-Ti-O systems*, Ph.D. Thesis, Uppsala University, Uppsala 2000, Acta Univ. Upsal. Abstr. Uppsala Diss. Sci. **594,** 47p.

79. Cho, Y.J., Min, Y.-S., Lee, J.-H., Seo, B.-S., Lee, J.K., Park, Y.S., and Choi, J.-H., Atomic layer deposition (ALD) of bismuth titanium oxide thin films using direct liquid injection (DLI) method, *Integr. Ferroelectrics* **59** (2003) 1483.

80. Min, Y.-S., Cho, Y.J., and Hwang, C.S., Amorphous high-*k* dielectric $Bi_{1-x-y}Ti_xSi_yO_z$ thin films by ALD, *Electrochem. Solid-State Lett.* **7** (2004) F85.

81. Min, Y.-S., Cho, Y.J., Ko, J.-H., Bae, E.J., Park, W., and Hwang, C.S., Atomic layer deposition of $Bi_{1-x-y}Ti_xSi_yO_z$ thin films from alkoxide precursors and water, *J. Electrochem. Soc.* **152** (2005) F124.

82. Min, Y.-S., Asanov, I.P., and Hwang, C.S., Effect of alumina addition on Bi-Ti-Al-O dielectric thin films, *Electrochem. Solid-State Lett.* **9** (2006) G231.

83. Honjo, T., Imura, H., Shima, S., and Kiba T., Vacuum sublimation behavior of various metal chelates of 4-Anilino-3-pentene-2-one, acetylacetone, dithiocarbamates, oxine and its derivatives, dimethylglyoxime, dithizone, 1-(2-pyridylazo)-2-naphthol, and tetraphenylporphyrin, *Anal. Chem.* **50** (1978) 1545.

84. Eisentraut, K.J., and Sievers, R.E., Volatile rare earth chelates, *J. Am. Chem. Soc.* **87** (1965) 5254.

85. Morozova, N.B., Igumenov, I.K., Mit'kin, V.N., Kradenov, K.V., Potapova, O.G., Lazarev, V.B., and Grinberg, Y.K., Zirconium(IV) complexes with β-diketones, *Russ. J. Inorg. Chem.* (Engl. transl.), **65** (1995) 963.

86. Putkonen, M., and Niinistö, L., Zirconia thin films by atomic layer epitaxy. A comparative study on the use of novel precursors with ozone, *J. Mater. Chem.* **11** (2001) 3141.
87. Putkonen, M., Nieminen, M., Niinistö, L., Niinistö, L., and Sajavaara, T., Surface-controlled deposition of Sc_2O_3 thin films by atomic layer epitaxy using β-diketonate and organometallic precursors, *Chem. Mater.* **13** (2001) 4701.
88. Putkonen, M., Sajavaara, T., and Niinistö, L., Enhanced growth rate in atomic layer epitaxy deposition of magnesium oxide thin films, *J. Mater. Chem.* **10** (2000) 1857.
89. Putkonen, M., Sajavaara, T., Niinistö, J., Johansson, L.-S., and Niinistö, L., Deposition of yttria-stabilized zirconia thin films by atomic layer epitaxy from β-diketonate and organometallic precursors, *J. Mater. Chem.* **12** (2002) 442.
90. Ylilammi, M., and Ranta-aho, T., Optical determination of the film thicknesses in multilayer thin film structures, *Thin Solid Films* **232** (1993) 56.
91. UniQuant *Version 2 User Manual*, Omega Data Systems, Neptunus 2, NL-5505 Velhoven, The Netherlands, 1995.
92. Putkonen, M., Sajavaara, T., Niinistö, L., and Keinonen, J., Analysis of ALD-processed thin films by ion-beam techniques, *Anal. Bioanal. Chem.* **382** (2005) 1791.
93. Putkonen, M., Nieminen, M., Niinistö, J., Sajavaara, T., and Niinistö, L., Surface-controlled deposition of Sc_2O_3 thin films by atomic layer epitaxy using β-diketonate and organometallic precursors, *Chem. Mater.* **13** (2001) 4701.
94. Matero, R., Rahtu, A., Ritala, M., Leskelä, M., and Sajavaara, T., Effect of water dose on the atomic layer deposition rate of oxide thin films, *Thin Solid Films* **368** (2000) 1.
95. Zhao, J.S., Sim, J.S., Lee, H.J., Park, D.-Y., and Hwang, C.S., Investigation of the deposition behavior of a lead oxide thin film on Ir substrates by liquid delivery metallorganic chemical vapour deposition, *Electrochem. Solid-State Lett.* **9** (2006) C29.
96. Hendricks, W.C., Desu, S.B. and Tsai, C.Y., Structure and kinetics study of MOCVD lead oxide (PbO) from lead bis-tetramethylheptadionate ($Pb(thd)_2$), *Mat. Res. Soc. Symp. Proc.* **335** (1994) 215.
97. Kosola, A., Putkonen, M., Johansson, L.S., and Niinistö, L., Effect of annealing in processing of strontium titanate thin films by ALD, *Appl. Surf. Sci.* **211** (2003) 102.
98. Nieminen, M., Sajavaara, T., Rauhala, E., Putkonen, M., and Niinistö, L., Surface-controlled growth of $LaAlO_3$ thin films by atomic layer epitaxy, *J. Mater. Chem.* **11** (2001) 2340.
99. Hwang, C.S., and Kim, H.J., Deposition of $Pb(Zr,Ti)O_3$ thin films by metal-organic chemical vapour deposition using β-diketonate precursors at low temperatures, *J. Am. Ceram. Soc.* **78** (1995) 329.
100. Veuillen, J.-Y., Gomez-Rodriguez, J.M., Baro, A.M., and Cinti, R.C., Adsorption and diffusion of single Pb atoms on Si(111)7 x 7 and Si(111)5 x 5 surfaces studied by scanning tunneling microscopy, *Surf. Sci.* **377-379** (1997) 847.
101. Lee, W., and Woo, J., Preparation of $PbZrO_3$ thin films by plasma enhanced metalorganic chemical vapour deposition, *J. Mater. Sci. Lett.* **22** (2003) 1677.
102. Madsen, L.D., Weaver, L., and Clark, A.J., The properties of lead titanate thin films produced by chemical vapour deposition, *Can. J. Phys.* **74** (1996) 580.

103. Kim, J., Tsurumi, T., Hirano, H., Kamiya, T., Mizutani, N., and Daimon, M., Preparation of bismuth silicate films on Si wafer by metalorganic chemical vapor deposition, *Jpn. J. Appl. Phys*. **32** (1993) 135.

104. Melin, G., Chartier, T., and Bonnet, J.P., Volume expansion during reaction sintering of γ-$Bi_{12}SiO_{20}$, *J. Eur. Ceram. Soc.* **20** (2000) 45.

105. Büngener, R., Pamler, W., and Gösele, U., Diffusion of Sr, Bi, and Ta in amorphous SiO_2 *Mater. Sci. Semicon. Proc.* **6** (2003) 43.

106. Ghoshtagore, R.N., Donor diffusion dynamics in silicon, *Phys.Rev. B* **3** (1971) 397.